Thesis for Degree of Doctor of Philosophy

Development and application of Time-of-flight secondary ion mass spectrometry (ToF-SIMS) for skin permeation studies

Marwa Al-Bayati Munem

UNIVERSITY OF
GOTHENBURG

Department of Chemistry and Molecular Biology
University of Gothenburg
Gothenburg, Sweden
2023

Cover picture: schematics of ionization process in SIMS for imaging skin tissue

Avhandling för filosofie doktorsexamen,
Göteborgs universitet

marwah968@gmail.com

ISBN: 978-91-8069-585-5 (PRINT)
ISBN: 978-91-8069-586-2(PDF)
Tryck: Stema specialtryck, Borås, 2023

Distribution:
Institutionen för kemi och molekylär biologi,
Göteborgs universitet
Box 200, SE-405 30 Göteborg

Trycksak
3041 0234

Development and application of Time-of-flight secondary ion mass spectrometry (ToF-SIMS) for skin permeation studies

Marwa Al-Bayati Munem
Department of chemistry and molecular biology
University of Gothenburg, Gothenburg, Sweden 2023

ABSTRACT

The skin accounts for approximately 16% of human body weight, with a surface area of approximately 2 m^2 in adults. It provides a physical barrier to the environment, maintains homeostasis by limiting the loss of water, electrolytes, and heat, and protects against microorganisms, toxic agents, and ultraviolet radiation. The outermost layer of the skin, the stratum corneum, serves as a first line of defense against volatile organic compounds, heavy metals, and other hazardous substances. Hence, understanding the skin uptake of environmental chemicals and particles is crucial for assessing the risks associated with pollution and for developing strategies to mitigate these risks. Moreover, elucidating the mechanisms of skin penetration by different pollutants and chemicals can contribute to the development of protective skincare products and other preventive measures.

Lipids in the skin are one of the main protective components and are crucial components of the stratum corneum where they play a significant role in the skin's barrier function. They fill the spaces between corneocytes and create a hydrophobic barrier that prevents the easy passage of substances, including chemicals and particles from the environment. The study of skin uptake and lipids changes in skin is of great interest in understanding underlying mechanisms of exposure to chemicals and environmental agents.

Mass spectrometry imaging (MSI) is a powerful label-free technique to study the skin composition as well as the link between lipid changes and the permeation of different chemicals. One of the most common MSI techniques is time of flight secondary ion mass spectrometry (ToF-SIMS), which provides ultra-high spatial resolution due the use of the focused ion beam to eject and ionize molecules in the sample surface.

The papers in this thesis describe the application of ToF-SIMS to investigate human skin tissue samples to reveal the permeation of metals and chemicals through the skin layers, as well as to study lipid changes caused by the uptake of these substances. Different sample preparation methods and different human skin samples and models have been examined to provide the best possible results. The method is now ready to be applied in testing pharmaceuticals, cosmetics, occupational skin hazards, and skin allergens independently or as a complementary approach to answer more complicated scientific questions.

***Keywords**: Mass spectrometry imaging, ToF-SIMS, lipids, skin, human skin models, toxicology, allergen, permeation studies, contact allergy, sunscreen, skin lipids, lipid change.*

Populärvetenskaplig sammanfattning

Huden är kroppens största organ med en yta på totalt ca 2 kvadratmeter. Huden fungerar som en första försvarslinje mot virus, bakterier och andra skadliga ämnen. Varje dag utsätts vår hud för en mängd olika kemikalier genom till exempel luftföroreningar, solkrämer, rengöringsmedel och konserveringsmedel. Men det har hittills inte varit möjligt att veta exakt hur huden tar upp dessa. Huden består av fler skikt och med hjälp av så kallad avbildande masspektrometri blir det nu möjligt att se alla skikt av huden och mäta närvaro av i princip vilka ämnen som helst, i vilken del av huden som helst.

Med avbildande masspektrometri kan vi mäta upptag av farliga ämnen och tekniken kan även utnyttjas för att utveckla exempelvis läkemedel som är bättre anpassade för huden. Avbildande masspektrometri innebär att man använder en laser eller jonstråle för att analysera hudsnitten med hjälp av en masspektrometer. I varje punkt, eller pixel, av snitten som strålen träffar får vi information det kemiska innehållet. Den kemiska informationen från varje punkt kan sedan samlas ihop till en digital bild som visar ett ämnes fördelning i huden. I den här avhandlingen har sekundärjonsmasspektrometri (ToF-SIMS) använts vilket ger en mycket hög rumslig upplösning ned till nanometerområdet.

ToF-SIMS metoden kan visa alla möjliga ämnen med en bild, oavsett om det är metall, ett solskydds kemiska innehåll eller ett toxiskt ämne man letar efter i huden, eller om man vill följa ett läkemedels väg genom huden. Det räcker med ett hudprov så kan man söka efter vilka molekyler som helst. Metoden behöver inte anpassas på förhand efter vad vi letar efter vilket gör metoden snabb och effektiv. Vill man veta något om den mänskliga hudens passiva upptag, så är ToF-SIMS den rätta metoden att använda sig av.

List of publications and contribution report

This thesis is based on the following studies

I. Munem, M.; Djuphammar, A.; Sjölander, L.; Hagvall, L.; Malmberg, P.
Animal- Free Skin Permeation Analysis Using Mass Spectrometry Imaging.
Toxicology in Vitro 2021, *71*, 105062.
https://doi.org/10.1016/j.tiv.2020.105062**.**

Participated in planning and designing the study, performed all the experiments together with co-authors, analysed and interpreted the data, made the graphs and figures and wrote major part of the manuscript. Responded to reviewer comments.

II. Hagvall, L.; Munem, M.; Hoang Philipsen, M.; Dowlatshahi Pour, M.; Hedberg, Y.; Malmberg, P.
Skin Permeation Studies of Chromium Species – Evaluation of a Reconstructed Human Epidermis Model.
Toxicology in Vitro 2023, *91*, 105636.
https://doi.org/10.1016/j.tiv.2023.105636.

Performed part of the experiments together with co-authors, took part in analyzing and interpreting the data, took part in making the graphs and figures and wrote major part of the manuscript. Responded to reviewer comments.

III. Munem M, Hagvall L, O'Boyle N. M. and Malmberg P**.**
Mass spectrometry imaging reveals methylisothiazolinone uptake in ex vivo human skin. Manuscript in preparation.

Performed all ToF-SIMS experiment, analysed and interpreted the data, made the graphs and figures and wrote a major part of the manuscript.

IV. Munem M, Hagvall L, O'Boyle N. M. and Malmberg P.
An evaluation of different skin models using ToF-SIMS imaging.
Manuscript in preparation.

Planned and designed the study, performed all ToF-SIMS experiment, analyzed and interpreted the data, made the graphs and figures and wrote major part of the manuscript.

Related publications not included in the thesis:

I. Phan, N. T. N.; Munem, M.; Ewing, A. G.; Fletcher, J. S. **MS/MS Analysis and Imaging of Lipids across Drosophila Brain Using Secondary Ion Mass Spectrometry.** *Anal Bioanal Chem* **2017**, *409* (16), 3923–3932. https://doi.org/10.1007/s00216-017-0336-4.

II. Munem, M.; Zaar, O.; Dimovska Nilsson, K.; Neittaanmäki, N.; Paoli, J.; Fletcher, J. S**. Chemical Imaging of Aggressive Basal Cell Carcinoma Using Time-of-Flight Secondary Ion Mass Spectrometry**. *Biointerphases* **2018**, *13* (3), 03B402. https://doi.org/10.1116/1.5016254.

III. Evenbratt, H.; Munem, M.; Malmberg, P. **ToF-SIMS Imaging of Dual Biomolecular Monolayer Gradients**. *Biointerphases* **2020**, *15* (6), 061014. https://doi.org/10.1116/6.0000621.

ABBREVIATIONS

MSI	Mass spectrometry imaging
ToF-SIMS	Time of flight secondary ion mass spectrometry
FA	Fatty acid
TAG	Triacylglcerol
DAG	Diacylglycerol
MAG	Monoacylglycerol
ER	Enodoplasmatic reticulum
PC	Phosphatidylcholine
PE	Phosphatidylethanolamine
PI	Phosphatidylinositol
PS	Phosphatidylserine
CER	Ceramide
SM	Sphingomyelin
CE	Cholesterol ester
SC	Stratum corneum
TJs	Tight junctions
Th 1	T helper cells type 1
Th 2	T helper cells type 2
ILC	Innate lymphoid cells
HPLC	High performance liquid chromatography
UV-VIS	ultraviolet–visible
LSC	Liquid scintillation counting
ICP-MS	Inductively coupled plasma-mass spectrometry
MS	Mass spectrometry
ESI	Electrospray ionisation
DESI	Desorption electrospray ionisation
MALDI	Matrix assisted laser desorption ionisation
RHE	reconstructed human epidermis

SIMS	secondary ion mass spectrometry
ToF	Time of flight
GCIB	Gas cluster ion beam
LMIG	Liquid metal ion gun
MD	molecular dynamic
COPD	Chronic obstructive pulmonary disease
MI	Methylisothiazolinone
SEM	scanning electron microscope
MVA	Multivariate analysis
PCA	Principal component analysis
PC	Principal component
MAF	Maximum autocorrelation factor

CONTENENTS

INTRODUCTION

Human skin is the largest organ of the body with a variety of advanced functions. It protects the body from xenobiotic and microbial attacks, helps regulate body temperature and permits sensations of touch, heat and cold. Skin also functions as a barrier that regulates the penetration of various compounds. Investigating how different substances pass into and through the skin is of great importance in different fields including studying skin diseases, drug and cosmetic development.

Chemical imaging is a very useful technique that allows us to see all layers of the skin with very high precision and to measure the presence of any substances in any part of the skin. Mass spectrometry imaging(MSI) is a label free technique which is becoming widely used to image biomolecules, drug and metal penetration in skin as well as localization in different organs[1–4]. The main advantage of MSI is the label free detection of large number of molecules within one experiment on the same tissue section allowing detection of both endogenous and exogenous compounds in parallel. Different MSI techniques have different characteristics especially when it comes to achievable lateral resolution and so far, Time of flight secondary ion mass spectrometry, ToF-SIMS, delivers the best possible, down to nanometer scale resolution. This is due to the advantage of using an ion beam as ionizer, and this can be focused to a small spot size.

In this thesis the imaging mass spectrometry technique that has been applied is ToF-SIMS. ToF-SIMS is a technique where a focused ion beam bombards a sample surface to eject material (secondary ions) that give us chemical information about the surface area. ToF-SIMS is an excellent method to study lipids and lipid changes in various tissues. Lipids are a group of substances that are found in all human tissues including skin tissue. They serve several essential functions in the human body. Changes in lipids and lipid metabolism causes various health effects in the human body including cancer, diabetes, obesity as well as neurodegenerative diseases. Changes in skin lipid composition are involved in different skin diseases including acne, atopic and seborrheic dermatitis[5,6]. Another unique ability of

ToF-SIMS is the ability to also provide information about the elemental composition of a sample and the ability to monitor metals and minerals in cells and biological tissues[4,7–9].

The aim of this thesis is to expand the application area of the ToF-SIMS imaging technique for lipid analysis of the skin tissue and to study permeation of different chemicals and allergens through the skin tissue using human skin biopsies, skin reconstruction and an ex-vivo human skin model. Finally, an evaluation of skin models using ToF-SIMS is performed to get a better understanding of similarity and differences between ex-vivo human skin and in-vitro human skin reconstruction to get a better understanding and interpretation of results collected by ToF-SIMS. The main goal of this thesis has been to advance the ToF-SIMS technique for different skin applications and to generate knew knowledge from the sample studied likewise taking a critical look at past research and the result validity using standard techniques.

Chapter 1

LIPIDS

Lipids is a general term used to refer to a group of substances that are insoluble in water but dissolve in non-polar organic solvents. They include fats, waxes, sterols, fat-soluble vitamins (such as vitamins A, D, E, and K), acyl glycerols and phospholipids. Lipids occur in all living organisms and serve an important role as a key component of the cell membrane. Lipids are also involved in various biochemical functions such as energy storing and cell signaling. Changes in lipids and lipid metabolism are associated with a number of diseases such as cancer, diabetes, obesity as well as neurodegenerative diseases[10–13]. The majority of the lipids are amphiphilic, they have a hydrophilic or polar head and hydrophobic or nonpolar tails, which make it possible to build the cell membrane in an aqueous environment[14].

Lipids classes and structures

Lipid structures are very diverse and thus there are different ways to classify them. A number of sources divide lipids into, simple and complex, based on their hydrolysis yielding, where simple lipids yield at most two types of primary products per mole, while complex lipids yield three or more primary hydrolysis products per mole. For example acylglycerol (fatty acid and glycerol) is simple lipid, while glycerophospholipids (fatty acid, glycerol and head group) are complex lipids[15,16]. Other sources add in a third group called derived lipids which contains alcohols and fatty acids derived by hydrolyzing simple lipids[17].

The International Lipid Classification and Nomenclature Committee on the initiative of the LIPID MAPS Consortium established a comprehensive classification system for lipids based on chemical and biochemical properties[18,19]. Based on this classification system, lipids have been divided into eight main categories: fatty acyls, glycerolipids, glycerophospholipids, sphingolipids, saccharolipids and polyketides, sterol lipids and prenols. Each category is

further divided into classes and subclasses. This section will not cover all lipid classes. It mainly focuses on skin lipids detected by ToF-SIMS.

Fatty acids (FA)

Fatty acids are carboxylic acids with a long hydrocarbon side chain. The chain can be saturated or unsaturated and can differ in length and number of double bonds (Figure 1.1). Fatty acids build ester bonds with glycerol and are then called esterified fatty acids or circulate freely in the plasma and are then called free fatty acids, in addition they can also be found as lipid membrane constitute. Fatty acids are an important energy source of fuel for animals as they yield large quantities of ATP when metabolized.

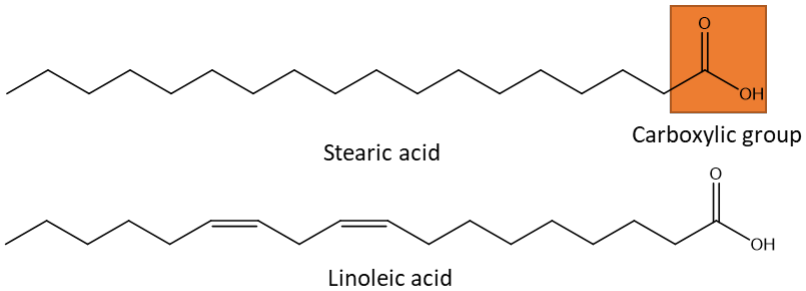

Figure 1.1. General structure of saturated FA, stearic acid FA (18:0) and unsaturated FA, linoleic acid (FA 18:2)

Glycerolipids

Glycerolipids are glycerol connected to fatty acids via an ester linkage. They can be mono-, di-, and tri-substituted, (Figure1.2). The position where the glycerol connects to a fatty acid is called the sn-position. They play a key role in membrane formation, caloric storage, and intracellular signaling processes.

Triglycerides (TAGs)

Triglycerides or triacylglycerols are glycerol esterified to three fatty acids via ester linkage. These mainly serve as energy storage as well as precursor for membrane lipid synthesis providing fatty acids and diacylglycerols. TAGs are mainly synthesized in the liver and stored in adipose tissue as lipid droplets wrapped in a monolayer of glycerol phospholipids decorated with proteins[20,21].

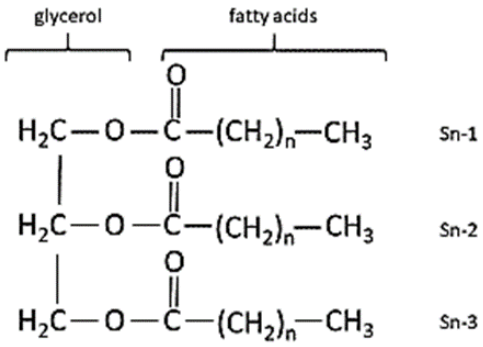

Figure 1.2 General structure of tri-substituted (triacylglycerol) glycerolipids

Diglycerides (DAGs)

Diglycerides or diacylglycerols are formed by esterification of two fatty acids to a glycerol backbone. DAGs are involved in a multitude of metabolic pathways. They function as components of cellular membranes, as building blocks for glycerophospholipids, and as lipid second messengers[22]. In the cell, DAGs can be either synthesized during de novo lipid biosynthesis or generated from other intracellular lipid species. The generation of DAGs occur in various subcellular compartments like the plasma membrane, the Golgi network, the endoplasmic reticulum (ER), and in lipid droplets[23].

Monoacylglycerol (MAGs)

Monacylglycerols are formed by the esterification of two fatty acids to a glycerol backbone. MAGs are generated by the hydrolysis of diglycerides. They are found at low levels in plants and animals and mainly serve as intermediates or signaling molecules.

Glycerophospholipids

Glycerol phospholipids or more commonly referred as phospholipids are the main structural component of biological membranes. They are highly amphiphilic, and this nature drives the formation of the lipid bilayer structure of membranes.

Phospholipids are formed from a glycerol backbone connected to two fatty acid tails (nonpolar part) and esterified with a phosphate group (the polar part) attached to the sn3-position of

the glycerol backbone. Depending on the polar head group structure, Glycerophospholipids can be divided into different subclasses with different biological function, see Table 1.1.

Phosphatidyl choline (PC)

Phosphatidyl cholines are a class of phospholipids that incorporate choline as the head group. The positively charged choline together with the negatively charged phosphate make PCs into zwitterionic molecules. PC lipids are the most abundant lipids in the mammalian cell membrane comprising about 50% of the total phospholipids pool and they dominate the outer leaf of the lipid membrane. PCs serve as precursor and signaling molecules for variety of signaling molecules including DAGs, phosphatic acids, choline and different lipases.

Phosphatidylethanolamine (PE)

Phosphatidylethanolamine is the second most abundant phospholipid in mammalian cells and is asymmetrically distributed across the cell membrane bilayers, but mainly enriched on the inner leaf. The positively charged ethanolamine head group together with the negatively charged phosphate group form a zwitterionic compound, and thus can be detected in both negative and positive ion mode with mass spectrometry.

Phosphatidylinositol (PI)

Phosphatidylinositol is a phospholipid that incorporates an inositol ring as the head group. Although it makes up a small fraction of the cellular phospholipids, PI has many key biological processes in the cell membrane, regulating ion channels, pumps and transporters. PIs make up about 10-15% of the total phospholipid concentration in mammalian cell membranes, and are found in the inner cell leaflet of the membrane. Since they carry several OH groups on the inositol ring, they are often observed in negative ion mode in ToF-SIMS spectra[24,25].

Phosphatidylserine (PS)

Phosphatidylserines are a class of phospholipids that incorporate serine as a head group substituent. They are minor phospholipids in the mammalian cell membrane, they can freely move between the membrane leafs. PSs have a key role in signaling during the early stage of apoptosis by stimulating the phagocytosis of the apoptotic cells and the production of anti-inflammatory mediators[26]. PSs are also co-factors that activate signaling proteins like protein

kinase C[27]. This group of phospholipids has less diversity of molecular species than PE and PC. PSs can be synthesized by replacing the choline head group on PC lipids or the ethanolamine on PE lipids[28].

Table 1.1. General structure of glycerophospholipid consisting of two non-polar fatty acid chain and phosphate group connected to different X-moieties.

Basic glycerophospholipid structure	**Substituten** X	**Chemical structure** X	**Glycerophospholipid**
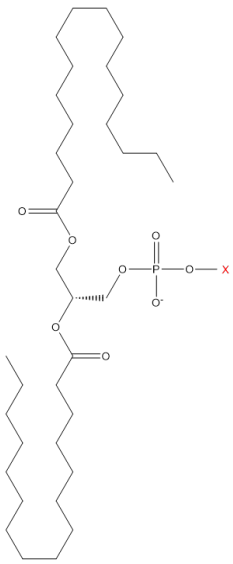	Hydrogen	— H	Phosphatic acid
	Choline	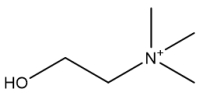	Phosphatidylcholine
	Ethanolamine	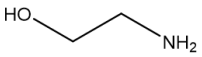	Phosphatidylethanolamine
	Inositol	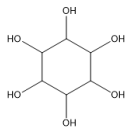	Phosphatidylinositol
	Serine	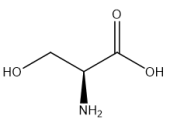	phosphatidylserine

Sphingolipids

Sphingolipids are lipids with a sphingosine base backbone connected to fatty acids via amide linkage and a head group at the primary hydroxyl, (Figure1.3). The head groups range from a simple hydrogen to more complex species, such as the phosphocholine moiety

of sphingomyelin. Sphingolipids are found in the outer leaf in all animals and function as structural components of membranes, lipoproteins, skin, and as cell signaling modulators and mediators[29].

Ceramides

Ceramides (CER) are the simplest sphingolipids, consisting of a sphingosine base connected to a fatty acid residue and having a hydrogen atom as a head group. Ceramides are the building blocks of all sphingolipids in mammals. In addition, they participate in regulating signal transduction, cell proliferation and apoptosis[30,31].

CER are found in high concentration in human skin membrane (in both inner-and outer-leaf). Ceramides are the major lipid constituent of lamellar sheets present in the intercellular spaces of the stratum corneum and thus involved in the barrier property of the epidermis[32]. Ceramides play an essential role in structuring and maintaining the water permeability barrier function of the skin, which makes it a common component in skin care products[33]. Alternation in ceramides metabolism is involved in many diseases such as cancer, diabetes and inflammation[34–36]. Ceramide can be synthesized *de novo*, from the condensation of amino acids. It can also be synthesized by the degradation of higher order sphingolipids.

Sphingomyelin (SM)

Sphingomyelin is a sphingolipid that consists of a ceramide with a phosphoryl choline moiety attached to the sphingoid base component. It is one of the most abundant lipids in mammalian cells, especially in myelin sheets covering the axonal part of the neuron. SM together with PC are the major lipids in the cell membrane and are found mainly in the outer leaf. Both lipids have a phosphocholine head group, consequently they are both zwitterions. Unlike the phosphatidylcholine with two fatty acids, sphingomyelin is attached to the sphingosine backbone with only one fatty acid. Sphingomyelin is primarily synthesized from two precursors, ceramide and phosphatidylcholine .sphingomyelin has important impact in cell signaling through its structural role in lipid rafts and also through its catabolic inter-mediators, such as ceramide and glycoceramid[37]. It is also involved in endocytosis and protein regulation.

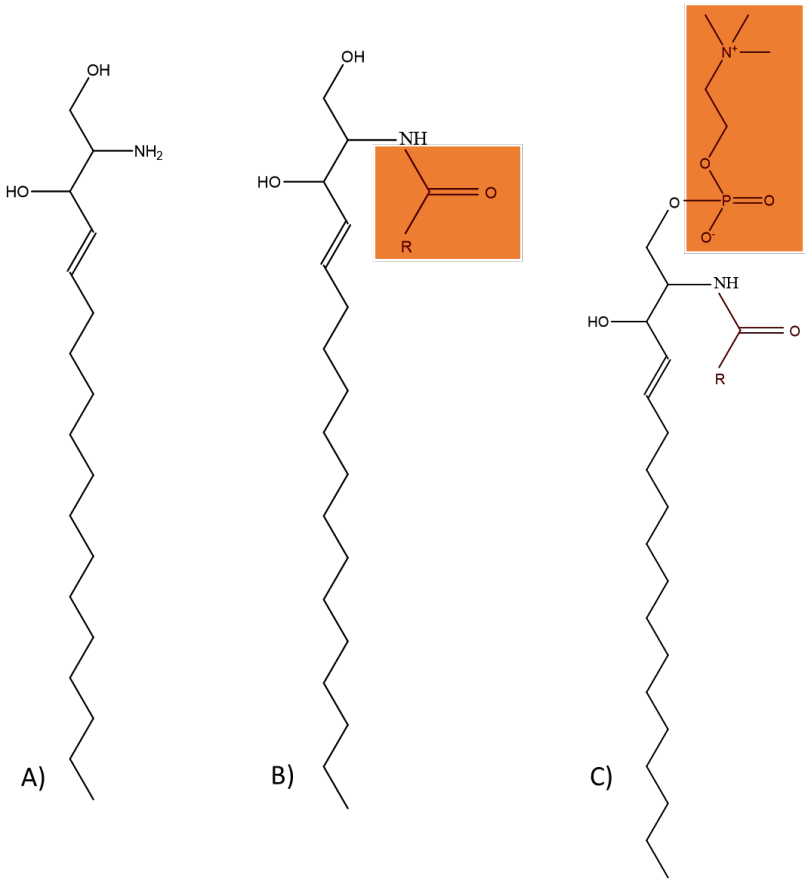

Figure 1.3. General structure of sphingolipids with sphingosine backbone.
A) sphingosine, B) ceramide and C) sphingomyelin

Sterols and Cholesterol

Sterols are lipids composed of cyclopentanoperhydrophenanthrene ring (composed of three six-carbon rings along with a five-carbon ring) with differing hydroxyl groups and side-chains, (Figure1.4). Sterols have been shown to influence fluidity and permeability of plasma membranes[38]. *Cholesterol* is a sterol composed of sterol four rings with a hydrocarbon tail and hydroxyl group. It is an essential constituent of the mammalian cell membrane, responsible for maintaining structure and fluidity. Moreover, Cholesterol serves as a building block for synthesizing various steroid hormones, including vitamin D, and bile acids.

Cholesterol also plays a crucial role in regulating cell function and cancer development[39–41]. Cholesterol is converted into cholesterol esters to allow transportation in the blood stream. Cholesterol esters are cholesterol with an ester bond formed between the hydroxyl group of the steroid structure and a fatty acid. Cholesterol esters (CE) function as a transport form of cholesterol in blood plasma and in cells in lipid droplets.

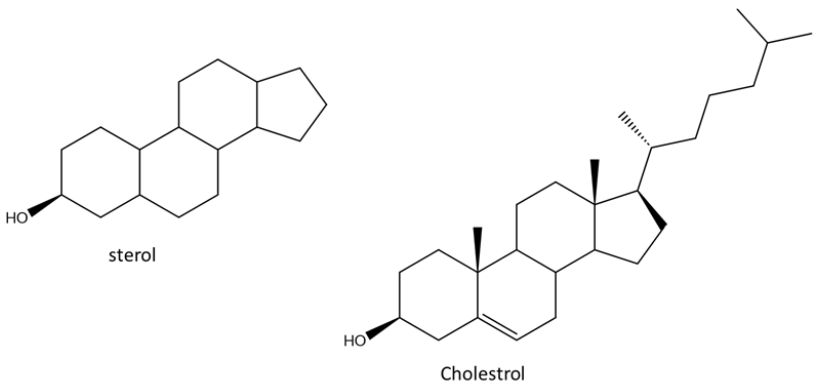

Figure 1.4. structure of sterol and cholesterol.

Lipids in skin

Skin lipids originate from either sebum or keratinocytes. Human sebum is a mixture of non-polar lipids, mainly triglycerides, wax esters, squalene, fatty acids and smaller amounts of cholesterol, cholesterol esters and diglycerides[6,42,43]. While , epidermal lipids (produced by keratinocytes) are a mixture of relatively equal proportions of free fatty acids, cholesterol and ceramides[44].

Human skin surface lipids consists of triglycerides, free fatty acids, wax esters, squalene, cholesterol esters, and cholesterol[45]. The epidermis contributes only for a proportion of the total surface lipid. In the lipid rich region such as the palm, sebum contributes to a big portion of the lipid continents. In the other hand, palms and soles where lipid production is less, lipids are mainly of epidermal origin[50]. Epidermal lipids, such as ceramides, triglycerides, and cholesterol, are integral components driving the formation and maintenance of the epidermal

permeability barrier as well as a barrier against microorganism invasion[46,47]. Although the main barrier functionality of skin is localized in the stratum corneum, sebaceous glands also serves as a mediator of the permeability barrier by providing photo protection and antimicrobial action[48].

The skin has one of the highest lipogenic activities of all tissues. Skin lipids have a wide variety of roles. They serve as sources of energy in the case of fatty acid oxidation, as a water barrier (e.g., ceramide), as growth regulators (e.g., arachidonic acid and prostaglandins), and as structural molecules in, for example, cell membranes.[49]. A balanced skin lipid composition is necessary for barrier integrity and stability, antimicrobial activity and pH maintenance[50]. Alteration in skin lipid composition is associated with inflammatory diseases, such as acne vulgaris, rosacea, atopic dermatitis, and psoriasis[51].

In this thesis lipids have been studied in human skin tissue after the exposure of different allergens and other chemical compounds. Hence I will examine human skin in more detail in Chapter 2.

Chapter 2

SKIN

Skin is the body's largest organ, covering its entire external surface and serving as a first-order physical barrier against external factors including bacteria, chemicals, and temperature. Moreover, it serves as an arena for diverse immunological processes, inflammatory processes, sensory receptors, water loss control, and homeostasis in general. The skin is also highly adaptive with different thicknesses and specialized functions in different body sites[52]. The skin accounts for approximately 16% of human body weight, with a surface area of approximately 2 m^2 in adults[53,54].

Human skin anatomy

Skin contains three main layers. the epidermis, the dermis, and the hypodermis. Hair, nails, sebaceous glands, and sweat glands (apocrine and eccrine) are considered to be skin appendages, (Figure 2.1).

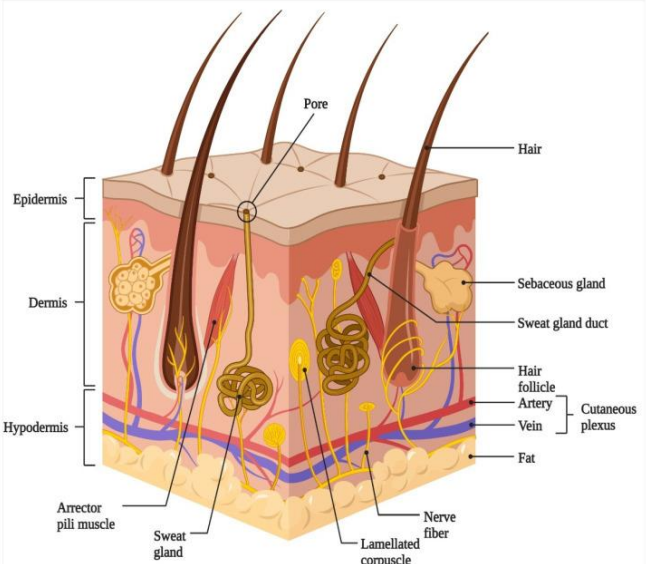

Figure 2.1. Schematic illustration of basic human skin anatomy showing the different skin layers and their components. Reprinted from Kolimi, P.et al. Innovative Treatment Strategies to Accelerate Wound Healing: Trajectory and Recent Advancements. Cells. 2022 Aug 6;11(15):2439. *Copyright © 2022, with permission.*

The epidermal layer is formed from squamous epithelium and is subdivided into separate layers, according to the degree of keratinization of the cells. The layers of the epidermis from the bottom to the surface are stratum basale (basal cell layer), the stratum spinosum (spinous or prickle-cell layer), the stratum granulosum (granular cell layer), and the stratum corneum (horny layer)[55], (Figure 2.2). Stratum lucidum is located between the stratum corneum and stratum granulosum and is only present in thicker skin such as palms and soles[56].

The stratum basale, stratum spinosium and the stratum granulosum form together the viable epidermis (thickness: 50–100 µm), whereas the SC (thickness: 10–20 µm) is part of the non-viable epidermis[57]. The cells of the epidermis include predominantly keratinocytes. It also includes melanocytes that produce melanin which protects against ultraviolet radiation, the Langerhans cells that are involved in immune functions, and the Merkel cells which plays roll in light touch sensation.[58]

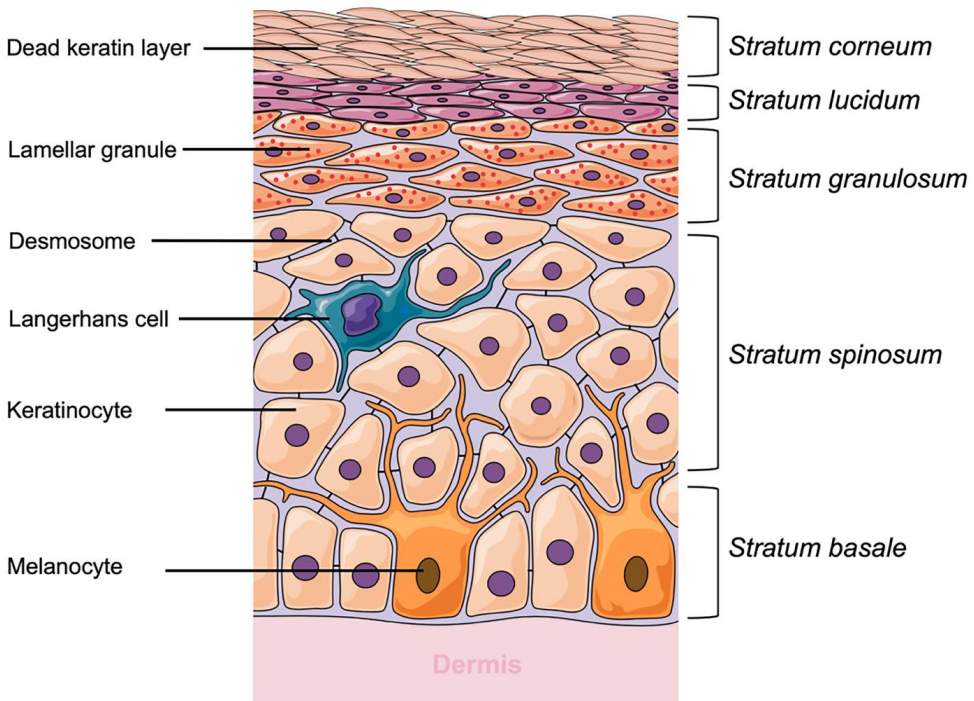

Figure 2.2. Schematic presentation of the human skin epidermis layers and their components. Reprinted from Ramadon, D. *et al.* Enhancement strategies for transdermal drug delivery systems: current trends and applications. *Drug Deliv. and Transl. Res.* **12**, 758–791 (2022). *Copyright © 2021, with permission.*

Lamellar granules or so called lamellar bodies are small organelles that first appear in the spinous layer, increase throughout the granular layer, and extrude their contents at the boundary between the granular layer and the stratum corneum. The lamellar granules contain several types of lipids (ceramides, cholesterol, fatty acids) and hydrolytic enzymes including proteases, acid phosphatases, lipases and glycosidases[59–61]. Desmosomes are intercellular junctions that mediate cell–cell adhesion and anchor the intermediate filament network to the plasma membrane, providing mechanical resilience to the epidermis. They also serve as a tool kit in modulating form and function of the epidermis.

Dermis is located between epidermis and hypodermis and is 1.5-4 mm thick. The dermis is divided into the papillary dermis and the reticular dermis. The papillary dermis is a thin superficial layer of the dermis lies beneath the epidermis and consists of collagen fibers, fibroblast cells, fat cells, blood vessels, nerve fibers, touch receptors and phagocytes. The reticular dermis hypodermis, also called subcutis or subcutaneous layer, is the deepest layer of the skin and consists of a network of fat and collagen cells. It conserves the body's heat as well as protects the inner organs. It also stores fat as an energy reserve for the body. The thickness of the hypodermis varies throughout the body and from person to person[62,63].

Dermal absorption

Dermal absorption occurs when a compound is taken up by the skin further to the rest of the body. Chemicals penetrate the stratum corneum by passive diffusion. Active transport plays a limited role in chemical transportation[64] and thus will not be discussed here. Chemicals pass through stratum corneum into the viable epidermis and continue passively through to the dermis via the dermal-epidermal junction the blood vessels will transport it to the systemic circulation[61,65]. For a substance to be transdermally absorbed, it first needs to pass the lipophilic stratum corneum and continue through a more aqueous layers, lower epidermis and dermis to the blood vessels. A lipophilic compound crosses the stratum corneum easily, but the penetration rate will decrease as it reaches the hydrophilic epidermis. The decrease in penetration rate will slow down the diffusion of the substance will slow down leading to a temporary deposition within the skin. When a substance accumulates in the skin instead of passing directly through to the bloodstream it is described as a reservoir. A reservoir can be

present in the stratum corneum, the viable epidermis or in the dermis[66]. The substance staying in the reservoir will either be released with a certain delay to the blood stream or travel back to the skin surface. Amphiphilic molecules with a small molecular size have the best permeability through the skin barrier[67]. Electrolytes on the other hand are difficult to absorb when they are applied in aqueous solutions. Ions create a field of stable hydration that increases the size of the diffusing component[68].

The factors that affect absorption includes skin integrity, site of action (from fastest to slowest: Scrotal>Forehead >Axilla ≥ Scalp>Back = Abdomen>Palm and plantar), compounds physiochemical properties, concentration and duration time. Molecules can permeate the skin through either the trans-epidermal pathway or through appendages, Figure (2.3). The trans epidermal pathway is divided into trans-cellular pathway where the where small hydrophobic molecules passes between the cells through the lipid matrix. On the other hand, the inter-cellular pathway allows small hydrophilic and moderate hydrophobic molecules to pass through. The trans-appendageal pathway occurs through hair follicles, sweat ducts and the sebaceous glands. The appendages cover about 1% of the total skin area and allow extremely challenging molecules to pass through, for instance big hydrophilic molecules. It is believed that the intercellular pathway is main passage that is used by chemicals and other compounds to penetrate skin[69–71].

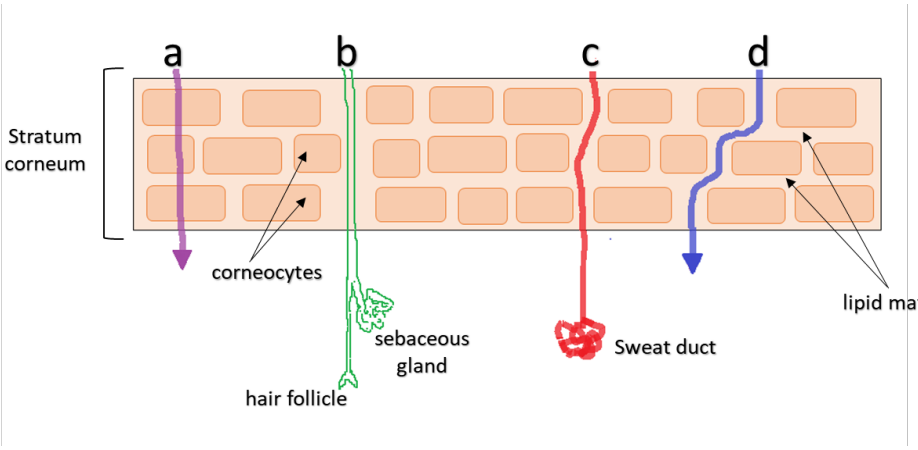

Figure 2.3. Schematic illustration of penetrations routes of a substance through passive diffusion a) inter-cellular pathway, b) and c) trans-appendageal pathway and d) intra-cellular pathway.

Skin barrier and inflammation

The epidermis contains two barrier structures, the stratum corneum (SC), which is unique to the skin, and tight junctions (TJs), which are present in other epithelial surfaces as well[72,73]. Both the SC and the TJs limit penetration of potentially toxic substances. A disruption in the skin barrier caused by a cut or penetration of a foreign body initiates skin inflammation.

Skin inflammation is a sign of an immune response in the body, to the potential toxic substances including allergies, infections, and autoimmune diseases. Skin inflammation can be classified as acute, often triggered by allergy or germs, and chronic caused by autoimmune disease like psoriasis. Acute inflammation is the initial response of the body to harmful stimuli. It starts by an increased movement of plasma and leukocytes in particular granulocytes from the blood into the injured tissues. A series of biochemical events occur and stimulates the inflammatory response, involving the local vascular system, the immune system, and various cells within the injured tissue. Prolonged inflammation, known as chronic inflammation, leads to a progressive shift in the type of cells present at the site of inflammation and is characterized by simultaneous destruction and healing of the tissue from the inflammatory process[74].

Inflammation is also classified as type 1 and type 2, based on the type of cytokines and T helper cells (Th1 and Th2) involved. Skin barrier disruption induces type 2 inflammation. Epidermal damage activates the innate immune response in a pro-inflammatory cascade. Skin barrier disruption permits access to external antigens by Langerhans cells and dermal dendritic cells, which present antigens to naive T cells and activate allergen-specific Th2 cells, leading to the release of the type 2 cytokines, IL-4 and IL-13[75,76]. It is now suggested that the chemokine CCL2 derived by residential skin cells and neutrophils is a main key driver in skin inflamation[77].

In response to barrier disruption and allergens, Keratinocytes and innate immune cells release chemokines that attract pro-inflammatory cells. Skin barrier disruption also stimulates keratinocytes to release alarmins that induce the type 2 innate lymphoid cells (ILC2s), Th2 cells, and basophils to release type 2 cytokines[78]. Type 2 inflammatory cytokines contribute to skin barrier disruption. In areas of active atopic dermatitis, type 2 inflammation leads to the

recruitment of additional innate immune effector cells, including eosinophils, basophils, and mast cell. These effector cells release mediators such as histamine that worsen skin barrier disruption by downregulating SC structural proteins and disrupting TJs[79,80].

Techniques to study skin penetration

The main methods to study skin penetration use a combination of vertical diffusion cells (this will be discussed in Chapter 4) with HPLC analysis of the fluid reservoir, UV-VIS spectrophotometry or Liquid scintillation counting (LSC)[81–84].

For both HPLC and UV-VIS spectrophotometry, the concentration of the substance is derived from a previously composed standard calibration curve. While, in LSC the measured substance is radio labelled and the amount of substance is measured by a scintillator counter.

Another method for drug quantification is tape stripping, that can also be combined with classical analytical methods such as HPLC[85]. Tape stripping is a relatively simple method where the formulation of interest is applied on a marked skin area and then an adhesive tape is pressed on the skin, followed by removal of the tape. The tape strips remove parts of the stratum corneum and amounts of any topically applied substances, for analysis. Despite the simplicity of this method, there are several parameters that can affect the result, including, site of application, type of tape, application of the tape strip, application pressure, velocity of removing the tape, quantification methods of the amount of SC removed, surface topography[86,87]. In addition, it is limited to study the penetration through the stratum corneum.

Inductively Coupled Plasma – Mass Spectrometry (ICP-MS) can also be applied to study metal permeation in skin[88–90]. With this technique localization of metals in the different skin layers is possible but the layers need to be separated prior to analysis.

All these approaches study how much of a compound penetrates the skin but typically do not address the distribution in the skin itself. The other common problem is the choice of acceptor media, which can give false conclusions because of solubility issues of the different chemicals[91].

The detection techniques that are routinely used to localize drugs in different compartments of skin are mainly imaging methods such as confocal microscopy or fluorescence

measurements[92,93]. These techniques require labeling of the substance, or are dependent on native fluorescence, which limits the number molecules that can be detected. Those limitations can be avoided by using mass spectrometry imaging as a complementary method to HPLC.

Mass spectrometry imaging(MSI) a label-free technique increasingly used to image the penetration of biomolecules, drugs, and metals in skin as well as in other organs[1–4]. The main advantage of MSI is the label free detection of large number of molecules within one experiment on the same tissue section allowing detection of both endogenous and exogenous compounds in parallel. Different MSI techniques have different characteristics especially when it comes to achievable lateral resolution and so far time of flight secondary ion mass spectrometry, ToF-SIMS, delivers the best possible lateral resolution for molecular imaging.[94,95]. Previously, in the field of dermatology, imaging mass spectrometry has been applied to study follicular transport of drugs in skin using DESI[1] and ToF-SIMS has been used to image basal cell carcinoma[96], age related lipid changes in stratum corneum[97], and mapping endogenous lipids in human skin[98]. MSI will be further discussed in a later chapter.

Human skin models

Skin models are experimental systems that mimic aspects of human skin physiology, function or disease. They include in vitro methods and ex-vivo skin cultures. In vitro skin models are important tool for studying different compounds penetration in human skin. It is a crucial step in the early phase of the development of pharmaceuticals and cosmetic products. Human skin tissues such as cadaver skin, biopsy material and surgical discards, provide the best possible model for such in vitro studies but the availability of human tissue is limited. In addition, there are a number of ethical issues concerning the use of human skin. Animal skin is another possible alternative, but the anatomical inter-species differences often compromise the translatability of animal based studies[99–101]. Moreover, the use of animals for gathering data for toxicological and cosmetic purposes is prohibited, according to the EU regulations[102]. Reconstructed human skin models have been widely used in drug testing, cosmetics and toxicology studies as an alternative to animal testing[103,104]. They are cell culture derived that usually consist of human keratinocytes and/or fibroblasts[105]. Several other skin cell types have

also been used in 3D bioprinted skin, including melanocytes, endothelial cells, pericytes, microvascular endothelial cells, follicle dermal papilla cells and also stem cells from various sources [106–108]. Despite the progress that has been made in the reconstruction of more complex skin models containing different cell types, there are still several tasks to tackle in order to model human skin in vitro mimicking all the structures and functions essential for skin research. The majority of published RHE models show a simplified two-layer setup, epidermal compartment represented by keratinocytes and dermal compartment represented by fibroblasts. While this set up is sufficient to reproduce the dominant structures and functions of the epidermis, a more accurate micro-architecture as well as a more diverse cellular composition would be needed to capture cell-cell, cell-matrix and dermal-epidermal signaling events. Other disadvantage when using in-vitro skin is the lack of the skin appendages, high cost and short shelf-life(up to one week) [109]. Human skin samples are always better alternative than a reconstruct and they can be kept alive in cultures for 4 weeks without losing the barrier function[110]. Hence, ex vivo skin models are robust enough to support toxicity and efficacy testing of pharmaceuticals, chemicals, and cosmetics. More relevant and comprehensive data can be delivered by the ex-vivo skin. Both reconstructed human skin epidermis and ex-vivo skin have been used in this thesis to examine the penetration and permeation of different compounds through skin. The RHE model used in this thesis Is a 3D tissue model consisting of normal, human-derived epidermal keratinocytes.

Chapter 3

MASS SPECTROMETRY

Mass spectrometry imaging (MSI)

Mass spectrometry imaging is a fast-developing analytical method, to analyze the surface of biological samples. MSI makes it possible to get information about the distribution of biomolecules in cells and tissues. It is the only analytical method that makes it possible to get the spatial distribution of virtually all biomolecules over a biological sample surface in a single run[111]. There are a wide variety of mass spectrometry imaging instruments. The main basic components that all mass spectrometers share are the ion sources, the mass analyzer, and the detector. The ion source, transfers molecular species to the gas phase and ionizes them[112]. The mass analyzer separates the ions according to their mass to charge ratio. The detector records the relative abundance of each ion, and the signal is recorded by a computer. The result is then presented in a plot of ion signal against mass to charge ratio (m/z), (Figure3.1).
The most common MSI techniques used in the analysis of biological materials are secondary ion mass spectrometry (SIMS), matrix assisted laser desorption ionization (MALDI), and desorption electrospray ionization (DESI). All three techniques have proven to be successful in lipid detection and imaging. The MALDI and DESI techniques cover a broader range of biomolecules (proteins, peptides, and nucleotides) which give them higher chemical specificity. SIMS on the other hand has higher spatial resolution and can visualize metals and elements, but covers a much smaller effective mass range of biomolecules, fatty acids and lipids[113–118].
All three techniques can deliver spatially resolved MS data in different ways on biological samples. In each case it is important to know the identity of the chemicals being sought and how that influences sample pre-treatment and analysis procedure. It is important to bear in mind, during data interpretation, the possibility of matrix effects on the ion signals observed.

For all three techniques the absence of signals cannot directly be translated as absences of chemicals. These techniques can provide information that chemicals are present, although signal intensities may be influenced by the presence of other chemicals so any sort of conclusions on relative concentrations must be taken with care. All three techniques can provide 2D image information, but the spatial resolution capability in 2D is dependent on the size of the probe used and the intensity of the signal obtained from the pixel size specified. SIMS is the only technique able to provide 3D images with nanometer scale resolution in the *z* direction. These three techniques can be selected for an application depending on how their particular strength matches the problem to be studied[119].

In some cases, it will be wise to apply more than one technique to provide complementary data delivered by each method[120–122].

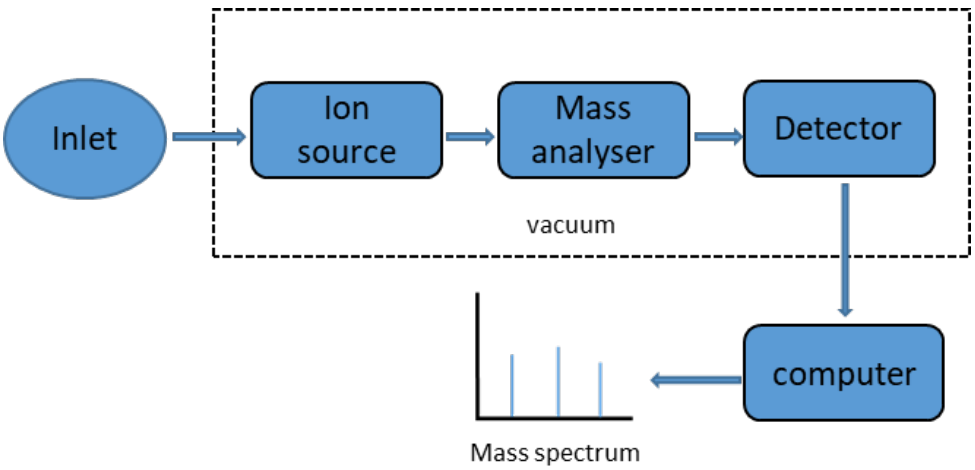

Figure 3.1. A schematic diagram showing the components of a mass spectrometer. The inlet device loads the sample into the ionisation chamber where the analyte is ionised by a suitable method and directed towards the analyser. In the analyser ions are sorted on the basis of their *m/z* value and are sent to the detector. Within the detector the ion flux produces an electrical current proportional to the number of ions reaching it. The processing unit records the magnitude of these electrical signals as a function of *m/z* and gives an output in the form of a mass spectrum.

Basic Principles of SIMS

Secondary ion mass spectrometry is a surface sensitive analytical technique that provides chemical information of a sample surface by applying a focused high energetic ion beam, so called primary ions, to sputter a surface. The sputtered materials ejected from the surface are both neutral and charged particles (Figure 3.2). It is only the charged particles, so called secondary ions, that can be detected and it is a very small fraction that correspond to less than 1% of the total sputtered material (at the so called static limit, see below). Sputtering is a term used to describe a phenomenon as energetic ions, atoms or molecules bombard a solid and thus leads to the ejection of particles out of the target from near the point of impact. The sputtered secondary ions carry information about the chemical composition of the sputtered surface[123]. The formation of the secondary ions, the so called ionization process, takes place at or close to the emission of the sputtered particles.

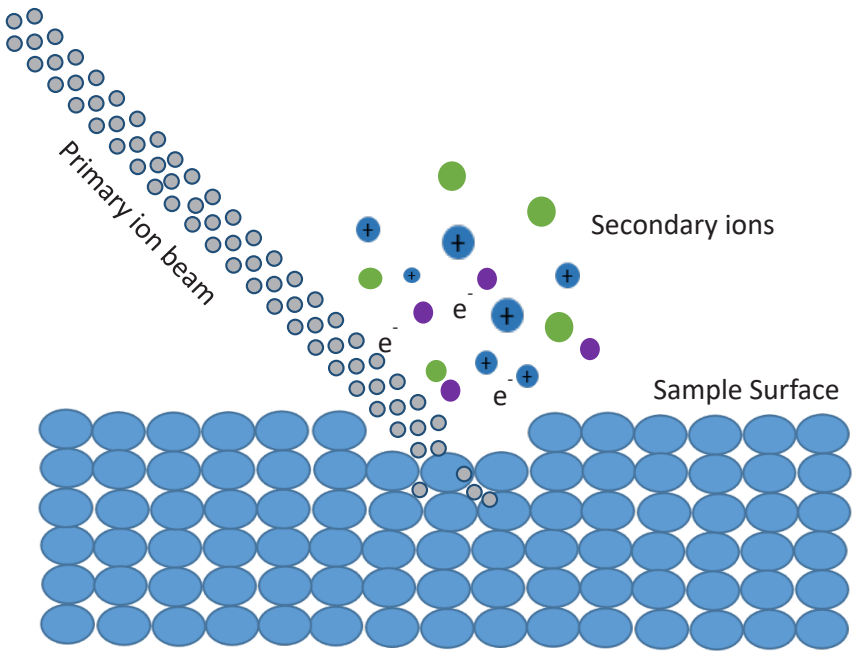

Figure 3.2. Schematic of the sputtering process in SIMS, where a focused ion beam bombards a sample surface and secondary ions, neutrals and electrons are ejected.

In order to understand the parameters that affect secondary ion yield, it is of interest to know the basic SIMS equation:

$$I_m = I_p\, y_m\, \alpha^{\pm}\, \theta_m\, \eta$$

where I_m is the secondary ion current of species m, I_p is the primary ion flux, y_m is the total yield of sputtered particles of species m, $\alpha^{\pm}$ is the ionisation probability to positive/negative ions, θ_m is the fractional concentration of the chemistry m in the surface layer, η is the transmission of the analysis system. The secondary ions generated in SIMS arise from the top layer of the sputtered sample; consequently, it is only the surface concentration θ_m that is relevant for the resulting secondary ions I_m.

The sputter yield includes all the secondary particles neutrals and charged increases linearly with increased primary ion dose, and also increases with the mass of primary ions, the energy applied and the incident angle of the primary ions[124,125]. The optimum beam energy to apply for maximal sputter yield lies between 5-50 keV[126]. The beam energy is limited by the instrument. The sputter yield as the name indicates, includes all the secondary particles both neutrals and charged species. The sputter yield and ionization probability can differ from one sample to another depending on the sample topography and roughness[125,127,128].

While sputter yield provides atomic information of the material under sputtering, **ionization probability** delivers chemical information about the secondary ions. The ionization probability indicates the fraction of secondary particles that are ionized[129]. The ionization process is not fully understood. Several theories have been suggested[130–133]. A simplified explanation for the ionization mechanism of molecular SIMS, is that ion emission is initiated by a momentum transfer processes, and some atomic and molecular species are sputtered by momentum transfer, while ion ejection occurs continuously. Within a dynamic region, known as the selvedge, extensive mixing occurs. Associations and disassociation reactions of the ions and molecules occur and lead to new ionic species including molecular ions, cat-ionized molecules, clusters, and fragment ions[134]. There are some properties that can affect the ionization. For example, the nature of the sample affects the ionization process, including the physiochemical properties of the sample i.e., electronegativity of the atoms in the compound, the ionic/covalent, morphology, etc. The ion yield varies greatly for the elements; the positive ion yield has a trend inversely dependent on ionization potential, and the negative ion yield has a similar trend, depending on electron affinity[135]. Environmental factors and target materials

also affect the ion yield. For example, a study showed that an increase of oxygen pressure in the analysis chamber, caused Si^+ ion yield to increase by 3 orders of magnitude during Ar^+ bombardment of silicon[136]. Another example is that the ion yield from an oxidized metal surface is much higher than that from non-oxidized metal surface[137]. The ionization probability is also affected by the primary ion beam used. Using a reactive primary particle such as O^- results in oxidation of the metal atoms in the impacted area thus increasing the ionization probability[138]. In general, SIMS detection efficiency for organic molecules is low and, yet, increasing ionization probability is crucial for expanding SIMS applications in this field[139–147]. Laser post ionization has shown to increase secondary ion yields[148]. Matrix enhanced secondary ion mass spectrometry is a method used to increase the ionization efficiency of high mass molecules[146]. Analyzing samples in a frozen hydrated state has shown to increase the formation of $[M+H]^+$ due to proton availability from the water clusters formed[149].

The ionization probability is highly dependent upon the material, or matrix, which surrounds the analyte, and the effect inhibits the ability to translate secondary ion intensities into quantitative measures of composition. Matrix effects cause enhancement or suppression of the ionization rate of an analyte in the present of other species and thus the secondary ion yield is not proportional only to the concentration of that analyte in the sample. Therefore, lacking internal standards, SIMS is not considered a quantitative but rather a semi-quantitative method. Semi-quantification can be performed by for example, comparing the signal intensities of a specific ion of interest in a sample to the intensity of the same ion in other samples[150,151].

The transmission of the analysis system is largely dependent on the instrument design used for the analysis and the adjustment of this parameter often requires exchange of components. In some instruments adjustment is more flexible but it results in uneven transmission for the analyte, i.e. transmission get enhanced for some analytes while decreases for others.

The static limit

An important consideration in SIMS is the static limit. In order for the analysis to reflect the nature of the undamaged 'static' surface, the sputtering process needs to be controlled so that statistically each primary ion hits an area only once, and that less than 1% of the top

monolayer of the sample is sputtered. This means that the fluence of primary ions is limited to a maximum of 1×10^{13} ions /cm^2, a value known as the static limit.

The development of large polyatomic primary ion beams and gas cluster ion beams has overcome this limitation to a significant extent in many materials, as these species provide very high sputter yields and do not penetrate the surface to the same depth, thereby leaving significantly less chemical damage in the sputter crater, allowing the static limit to be overlooked.[152,153]

Different SIMS modes of operation

There are two operational modes in SIMS, based on the fluence of the primary ions and the mass analyser: static SIMS and dynamic SIMS[154,155].

Static SIMS represents acquisitions with primary ion fluencies below 10^{13} ions/cm^2 (due to static limit). Hence, less than 1 % of surface molecules are affected and the primary ion beam will not bombard any area more than once , ensuring that the signal is coming from the original species and not as a result from reaction between ions and the non-sputtered molecular fragments.[156] Static SIMS instruments typically employ pulsed primary ion sources with an energy range of a few keV to tens of keV while using ToF mass analyzers. The ion sources are often poly- or clustered ion sources, generating molecular ions and larger fragments. Thus, they are more suitable for studying biological tissues[157]. ToF-SIMS instruments can be used to obtain chemical and spatial information as a function of depth; however, they are unable to collect data during the sputtering process. Depth profiles are obtained by continuously alternating between data acquisition and sputtering cycles, resulting in low duty cycle depth profiles.

Dynamic SIMS uses a higher fluence of primary ions (few tens of keV) to bombard the sample surface and chemical information is often acquired as a function of depth. This makes dynamic SIMS a highly destructive method. Dynamic SIMS uses continuous primary ion beams (usually Cs^+, O^-) and often applies scanning-based mass analyzers (magnetic sector). The continuous generation and detection of secondary ions results in high duty cycle acquisitions. Although instruments with scanning-based mass analyzers are able to continuously monitor secondary

ion generation during sputtering, they are limited in the number of ions detected per depth profile[158–160]. The main application areas for this method is studying elements, semi-conductors and geological sciences[161].

SIMS instrumentation

A basic SIMS instrument consists of:

- A primary ion beam source to supply the bombarding species
- Target or sample that must be solid and stable in a vacuum
- A method for collecting the ejected secondary ions
- A mass analyzer to isolate the ion of interest
- An ion detection system to record the magnitude of the secondary ion signal (photographic plate, Faraday cup, electron multiplier or a CCD camera and image plate).

Here I will discuss the mass analyzer and the primary ion beam source in more detail.

Mass analyzers

The mass analyzer in SIMS plays a crucial role. There are three types of mass analyzers that are mainly used in SIMS instruments. Quadruple, magnetic sector and Time-of-Flight. The quadrupole basic principle in mass spectrometry (MS) is to separate and detect masses by letting oscillating ions pass through the quadrupole to reach a detector. Quadrupole mass spectrometry is the simplest and most affordable. The limitations of quadrupole analyzers are the low mass resolution (< 3000) and poor mass accuracy (> 100 ppm) [162]. The magnetic sector analyzers use a magnetic and or electrostatic field to separate ions of different *m/z* values at a mass resolution of about 10,000 and with an accuracy of less than 10 ppm.

The Time of flight mass analyzer separates the ions in a field-free drift path according to their velocity. Previous ToF-SIMS instruments utilized time-of-flight analyzers with parallel-plate ion mirrors or toroidal ion mirrors, providing moderate mass resolution (<10,000) and accuracy (for low mass, 60 ppm). The introduction of reflection technology has significantly improved the mass resolution to about 13,000 and provided a better mass accuracy to ca 10 ppm[163].

In recent years, hybrid mass analyzers have been increasingly used in ToF-SIMS. an integration of a quadrupole and a ToF mass analyzer can be applied[164,165], where the quadrupole mass

analyzer is used to pre-select ions within a certain mass range before entering the ToF mass analyzer. By pre-selecting specific mass ranges using the quadrupole mass analyzer, the ToF-SIMS analysis can focus on the species of interest, resulting in improved signal-to-noise ratio and reduced interference from other species. This approach is particularly useful for analyzing complex samples such as biological tissues. Another type of hybrid mass analyzer combines ToF and Orbitrap mass analyzers[166], where both analyzers share the same secondary ion extraction optics and consequently analyze the same point on the sample providing high speed and high mass resolution , about 150,000 at *m/z* 200 with an acquisition rate of >20 spectra/s in a broad range of ions. This hybrid mass analyzer makes it a great tool for analyzing metabolites within biological samples.

Time of flight (ToF) mass analyzer in detail

The ToF mass analyzer separates the ions based on the fact that in a field free path, ions with the same *m/z* have the same velocity. The secondary ions formed by the sputtering process get accelerated into a flight tube (field free zone), where they are separated by differences in their velocities. The lighter ions travel faster than the heavier ions. The velocity of an ion in a flight tube is directly proportional to its mass and inversely proportional to its charge. The relationship between the ions m/z and the time it takes for it to travel through the tube can be derived from the potential energy equation together with the kinetic energy equation of the charged particle[167].

The potential energy, E_P, of a charged particle in an electric field can be described in the Equation below:

$$E_P = qV$$

where q is the charge of the ion and *V* is the acceleration potential (the strength of the electric field).

When an ion with a mass *m* and a charge q is accelerated by a potential *V*. The electric potential energy is converted into kinetic energy *E*.

$$E = \frac{1}{2} mv^2$$

Where m is the mass of a particle, and v is the velocity of the particle.

Since all potential energy is converted to kinetic energy we can combine both equations and expressing velocity as distance (length of the flight tube), *L*, divided by time, *t*, the following equation is produced:

$$\boldsymbol{t = \frac{L}{\sqrt{2V}}\sqrt{\frac{m}{q}}}$$

Both *L* and *V* are dependent on the instrument and therefore can be assumed to be constant value *K*. The equation can be written as

$$\boldsymbol{t = K\sqrt{\frac{m}{q}}}$$

The equation shows that the time it takes an ion to travel through a flight tube depends on the square root of mass to charge ratio.

This equation assumes that all ions enter the flight tube with the same kinetic energy. In reality, there is a different range of initial kinetic energy in the emitted ions with the same masses. The energy distribution is due to sample topography. This broad energy distribution leads to low mass resolution of the secondary ions[128]. The development of the reflectron, (Figure3.3) also called ion mirror, helped to improve the mass resolution by correcting the kinetic energy dispersion of the travelling ions[168]. Usually, a reflectron consist of a field free region and an ion mirror. As the secondary ions enters the mass analyzer they get accelerated in a potential field and then travel towards the field free region where the mirror is located at the end of the flight tube. The ions get reflected by the mirror, travels back into the field free region with new energy and a different angle and finally reach the detector. If the ion mirror of a reflectron consists of evenly spaced electrode plates that can have a single electric field region, then the reflectron is a single staged. The single-stage reflector utilizing a homogeneous field can be applied where the variation of energies of ions leaving the ion source is small. In contrast, the dual stage reflectron uses an ion mirror with two regions (stages) with different fields. Typically, the first part has high electric field followed by lower field where ions get repelled to the first region. This arrangement can compensate flight times over larger variations in ion kinetic energy compared to single-stage reflectron.

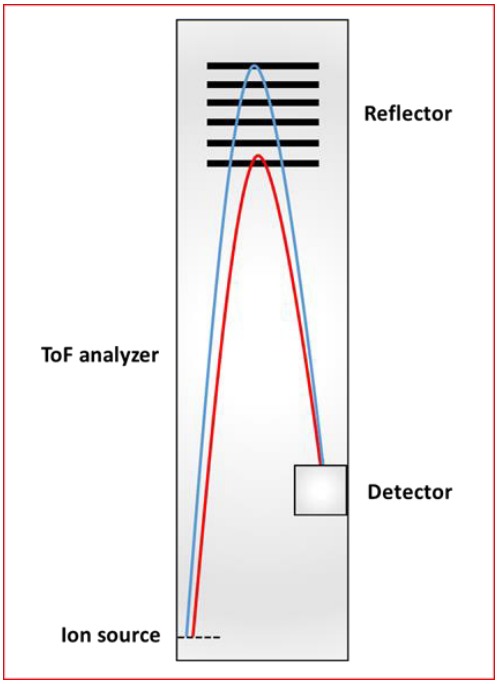

Figure 3.3 Schematic representation of a ToF analyzer with a reflector. Ions with low kinetic energy (red) penetrate only a short distance into the reflector, while ions with higher kinetic energy (blue) penetrate deeply into it.

Primary ion beams

Most static SIMS instruments applied atomic primary ion beams such as Ar^+, In^+, and Ga^+ until the beginning of the 21st century. These atomic ion beams have high energies, which allow the beam to penetrate deep into the sample analyzed and cause chemical damage. As a consequence, the molecular species disappear and get replaced by fragments that are uncharacteristic of the original chemistry of the sample being analyzed. In contrast, rastering the easily focused liquid ion beams that are generated from liquid metal sources, such as Ga^+, over a solid surface gives two dimensional chemical images with high spatial resolution. When primary ion beams are used, the static limit should be maintained and as a consequence the useful ion yield for the sub µm image resolution was very low.

Generally; however, the efficiency of secondary ion formation particularly that of complex molecular species is significantly enhanced with polyatomic ion beams instead of atomic species.

It was demonstrated in the 1990s that it is beneficial to increase primary ion nuclearity[169], but no primary ion beam had been developed for this purpose at this time. The interest of using heavier ion metals and cluster beams generated from liquid ion sources was growing again and Manchester University in a collaboration with Ionoptika developed a liquid gold ion gun that delivered 20 keV ions in high yield. At the same time IONTOF introduced the Bismuth ion gun[170,171]. The cluster ion beams Au_3^+ and Bi_3^+ provided a very high increase in signals especially in higher mass region, compared to Ga^+ ion beams due to a larger proportion of larger molecules emitted. The static limit requirement still applies, so the ionization probability is still the same although there is some evidence of increased ionization probability but the main reason for the high signal is due to higher sputter yield[172].

Apart from the sensitivity increase, cluster ion bombardment also appears to allow for molecular depth profiling studies without the accompanying damage accumulation normally associated with atomic projectiles. It appears that much of the benefit associated with cluster bombardment is connected to the fact that these projectiles give access to very high sputter yields which are not accessible with atomic primary ions, (Figure 3.4).

Gas cluster ion beam development for processing surfaces dates back to the 20th century. Industrial applications of cluster ion beams did not start to be explored until commercial equipment was first introduced to the ion beam community in around 2000[173]. The use of a cluster ion sources in a secondary ion mass spectrometry (SIMS) apparatus for the analysis of surface composition was investigated by experiments and by MD simulations in 2001[174]. About ten years later, the production of gas cluster ion beams, GCIBs was announced. GCIBs are now routinely used for low damage etching of samples for SIMS and also as analysis beams. Low energy GCIBs have low ionization efficiency of secondary ions, but they provide an increased signal in intact lipid regions in comparison with C_{60} beams which already have been shown to provide increased signals in comparison to other atomic and polyatomic ion beams[175]. GCIBs provide a significant reduction in the chemical background noise in comparison to C_{60}[176]. The disadvantage of Using GCIB as primary ion gun is a reduction of secondary ion yield and lower lateral resolution in comparison to C_{60}^+[141]. However, a deposition of C_{60}^+ can occur on the surface when used with higher energies (higher

than10KeV)[177]. For argon cluster ion gun, no apparent deposition on the surface have been noticed with higher energies (20 keV), and a high increase in the sputter yield have been noticed[178].

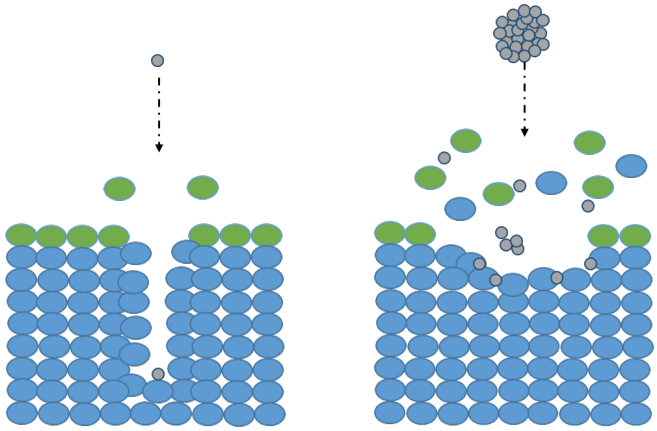

Figure 3.4. Comparison between a monoatomic ion beam (to the left) and a cluster ion beam, showing the differences in sputter yield and penetration depth. The mono atomic beam results in high penetration depth and less sputtered material. While the cluster ion beam causes less penetration damage to underlying layers and more material are sputtered.

ToF-SIMS imaging

Mass spectrometry imaging involves generating spectra from each specific pixel point on a sample surface using a focused ion source to ablate material and a chemical map of the sample surface is generated by assembling all the pixel data. ToF- SIMS provides the ability to focus the ion beam down to a very small spot size, thus, allowing high spatial resolution. Two different modes of detection are possible for ToF–SIMS imaging. In the microprobe configuration which is the main mode used (Figure 3.5), mass spectra a collected from a pre-selected pixel array and images are rebuilt retrospectively from an extended raw data set. The spatial resolution in this mode is dependent on the spot size of the ion source.

In contrast, the microscope mode uses a defocused ion source so that a large area is ablated and secondary ions are transported to the mass spectrometer with spatial distribution

maintained. Secondary ion distribution is magnified before detected at a position sensitive resistive a detector[179]. The spatial resolution here is dependent on the position sensitive ion detector instead of the spot size of the ion beam. The drawback with this mode is that simultaneous measurement of the spatial information and the time-of-flight of different ions is not possible. To obtain the spatial localization of multiple analytes, the sample analysis has to be repeated for each desired analyte[180]. Hence, this approach is less suitable for the analysis of biological tissues.

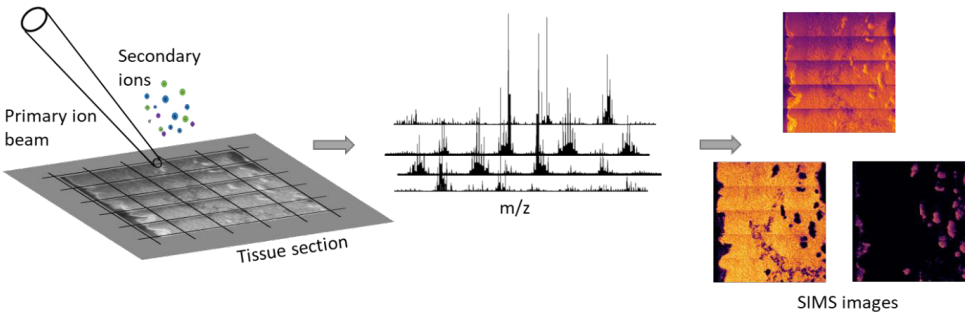

Figure 3.5. Schematic showing the microprobe imaging mode of ToF-SIMS. The ion beam is rastered over a sample surface to ablate the material from a pixel point on the sample and secondary ions are generated. One spectrum for each pixel point is generated, and these spectra are summed in a total mass spectrum. the intensity of each ion can be plotted against m/z ratio. Finally, a chemical map is created where it is possible to see exactly where each ion is localized.

Depth profiling (3D imaging) of biological tissues is also possible in ToF-SIMS. The most commonly employed approach in ToF-SIMS instruments is the dual beam mode, where an alternation between two ion sources is applied[181,182]. One ion source is used for etching the sample and the other one is used for the actual analysis. The analysis beam applied is usually a liquid metal ion gun, due to the ability to focus down to nm spot size and creates a regular 2D image. The sputter beam is usually a poly atomic or GCIB used to clean the sample surface stripping away layers and the alternation between cycles is continuous. The 2D images are then fused together in sequence and a 3D image is created. Despite the simplicity of the 3D imaging, there are factors to take into account when evaluating the data. These issues include surface topography, differences in sputter rates of materials, matrix effects, surface damage, and shifting of images due to changes in the sample height from material removal[183].

Other approaches that are used in SIMS for depth profiling are for example eroding the sample with one ion beam, which is mainly applied in Nano-SIMS analyzing semi- conductors. Another procedure is to perform a 2D imaging to image a series of consecutive sections that are pre marked. The images are then fused together [184].

Bioimaging with ToF-SIMS

ToF-SIMS is a powerful imaging tool for studying biological samples, due to the ultra-high sensitivity, specificity and high spatial resolution offered by this technique. ToF SIMS has been applied to image biological samples since the late 1990s[185]. The instrument advancements including the development of new primary ion sources and mass analyzers led to improved capabilities of ToF-SIMS for studying biological samples at the sub-cellular level. The ability of ToF-SIMS to detect diverse molecules in situ, and the ability to image with high spatial resolution, makes it exceptional tool for analyzing single cells[186,187]. It has been successfully applied to study cellular heterogeneity and function at single cell level[188–190]. Another application in single cell imaging is to study drug uptake and the interaction between drug molecules and the cell. In a study performed on macrophages, the uptake of the antiarrhythmic drug (amiodarone) and its metabolite were investigated. It was found that both the drug and its metabolite were present in the cell membrane and the subsurface region, while being absent in the nucleus. This study showed the mechanism of cellular uptake and distribution of pharmaceutical compound, providing the basis for studying cellular uptake of pharmaceutical compounds and their metabolites on the single cell level[191].

ToF-SIMS can also be applied to study lipidomics, due to the ionization and sputtering properties of ToF-SIMS and that the lipids are in a mass range that is detectable for this technique. ToF-SIMS has been successfully used to map lipids and elucidate lipid changes in different tissues, including skin, kidney, brain, heart, breast and liver[98,192–196]. ToF-SIMS imaging has been used to investigate lipid alteration in response to two drug treatments in Drosophila melanogaster brain tissue. Significant changes in phospholipid composition were observed in the central brain. Lipid changes occurred mainly for phosphatidylcholines, phosphatidylethanolamines, and phosphatidylinositols. When the lipid changes caused by the two different drugs were compared, it was shown that these drugs exert opposite effects on the brain lipid structure[197].

The ability of ToF-SIMS to image low-mass molecules with high sensitivity and specificity has made it possible to study metabolites such as sugars, amino acids and nucleotides[198,199].

ToF-SIMS can reveal complex metabolic processes and interactions that may be difficult to detect using traditional metabolomics techniques, for example, TOF-SIMS in combination with immunofluorescence was used to directly visualize metabolite distribution in different cell types, to find potential biomarkers for cell type classification[200].

ToF-SIMS also has the ability to detect elements in biological tissues[201]. ToF-SIMS was used to visualize and relatively quantify iron accumulation in lung tissue sections of healthy donors versus chronic obstructive pulmonary disease (COPD) patients. It was demonstrated that ToF-SIMS can be successfully employed to image iron distribution at cellular level in human lung tissue sections, and that iron levels were twelve times higher in lung tissue sections from COPD patients compared to healthy donors. Most of this iron was shown to be heterogeneously distributed within the iron-positive cells, consistent with accumulation within discrete cellular organelles such as mitochondria or lysosomes[4].

The ability to detect both organic and inorganic compounds during the same analysis makes ToF-SIMS a suitable technique for bone studies. ToF-SIMS is able to visualize and differentiate different areas of the mineralized bone as well as non-mineralized based on the chemical composition, with a high spatial resolution[202–205].

The examples listed here show that ToF-SIMS is a versatile and powerful tool that can be applied in many biological applications; however, there are still some limitations and aspects to be improved. The chemical complexity of biological samples can be challenging, distinguishing between different molecular species. Hence, a higher mass resolving power is needed for some applications. With the development of polyatomic ion sources and GCIB ion sources, more data is generated, making the data more complex to interpret, thus more specified multivariate data analysis are needed. More accurate spectral libraries are also needed for the identification of molecular species.

Another aspect for further improvement is the optimization of the sample preparation. For successful ToF-SIMS analysis of a biological sample, an optimized sample preparation is always required to ensure the preservation of the biological structures and that no artifacts are introduced. Poor preparation method can give false interpretation of the result (discussed in more detail in chapter 4).

Chapter 4

METHODS

Skin models

In this thesis three different skin models have been used in order to study the permeation of different metals and chemicals and also lipid composition and/or lipid changes in the different skin tissues. For studying sunscreen permeation in skin, a fresh frozen skin tissue from breast reduction surgery discard was used (paper I). For studying Cr^{III} and Cr^{VI} permeation, the previously mentioned skin tissue as well as reconstructed human epidermis were used (paper II). Ex-vivo human skin model was used to follow the permeation and the lipid changes owing to the application of the low molecular allergen methylisothiazolinone (MI), (paper III). the reconstructed human epidermis and ex-vivo human skin model were used in the evaluation study of different skin models.

Diffusion cells

The principle of a diffusion cell apparatus or Franz cell is based on in-vitro diffusion. The Franz vertical diffusion cell is the most commonly used instrument for the dermal drug testing for in-vitro permeation tests[206]. The first description of the method is named after Thomas J. Franz[207]. Basically, it consists of two compartments, a donor compartment (top chamber) and a receptor compartment (bottom chamber), separated by a membrane e.g. skin or skin equivalent. The sample is introduced at the top through the donor compartment, (Figure 4.1). The receptor compartment contains fluids from which samples are extracted over a time interval. The sample collected determines the amount permeates through the membrane. The receptor compartment of a diffusion cell or Franz cell has a fixed volume, and this allows the stirring of both the receptor and donor chamber[208]. In a flow diffusion cell, the receptor medium is circulated at the bottom from which samples are extracted for analysis over a time interval[209]. In a static diffusion cell, the medium is stirred using a magnetic stirrer. The receptor medium can be any fluid of interest with regard to the observed substance. Phosphate

buffered solution (PBS) is predominately used, since it closely mimics body fluid in terms of pH and salt contents[210].

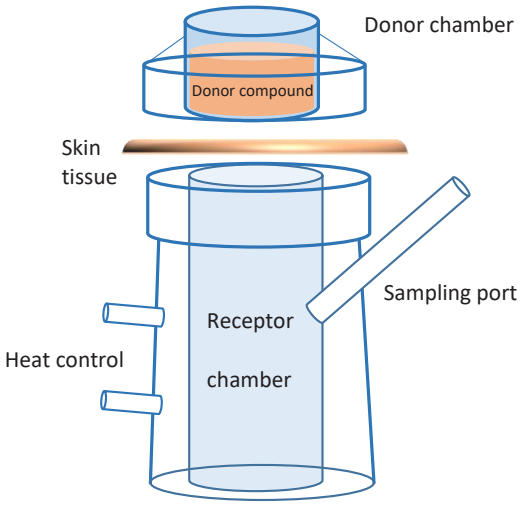

Figure 4.1. Schematic illustration of a Jacketed vertical static Franz diffusion cell used for transdermal penetration studies. The donor compound is introduced to the skin the donor chamber. The permeated substances are then collected in the receptor chamber that is prefilled with appropriate receptor medium.

Typically, the cell is held at a constant temperature that is appropriate for skin, or for body conditions[211]. This can be done by using a jacketed cell where water is circulated outside the receptor chamber. The extracted samples from the donor and/or receptor medium can be estimated with different analysis techniques that were mentioned earlier. The jacketed vertical diffusion cell has been used in the exposure experiments in paper I, II and III. The skin tissue used in paper IV was received pre-mounted by the company's in-house diffusion cell.

Sample preparation for ToF-SIMS

ToF-SIMS is a label free technique and does not need any sample pre-treatment. The main requirement is that the studied sample needs to withstand vacuum. Biological samples contain large amounts of water and thus pre-treatment is needed to make them vacuum compatible, whilst maintaining the sample integrity. Chemical fixation is a well-established

preparation method, and it has been widely applied in other high vacuum techniques, such as scanning electron microscopy. Chemical fixation employs agents which permeate tissues and cells and combine covalently with their major biochemical constituents (lipids, proteins and carbohydrates) and fix them into place and thus preserve structural integrity. It is possible to analyze chemically fixed samples, but a big part of the chemical information will be lost[212]. Cryopreservation is a physical fixation method where the sample is frozen using a cryogenic liquid followed by a drying step. Cryofixation is a suitable preparation method for ToF-SIMS analysis[213]. However, three problems could occur during this process. The first problem is formation of salt crystals and salt migration to sample surface. Salt crystals and other interferences can be eliminated by washing the sample with a volatile buffer salt such as ammonium acetate and ammonium formate prior to drying. The best washing solutions to use are volatile buffers such as ammonium acetate and ammonium formate[214,215]. The relative volatility of these buffers allows any residue remaining after the drying procedure to evaporate. The third problem that could occur during freeze drying is re-localization of some lipids due to the loss of water during the drying process. Changes of the distribution or a migration of some ions have been noticed in fly brain tissue during the freeze-drying procedure[192,192,216]. The third problem is water crystal formation during the freezing process. Ice crystals cause molecular displacement and thus sample structural changes. Large crystal formation can be avoided using the plunge freezing, where the sample is immersed in liquid nitrogen cooled cryogen, such as propane. High pressure freezing is another approach that can be applied to convert the samples water content into amorphous ice. The freeze-dried sample preparation can be used in all ToF-SIMS imaging instruments. Some instruments have the ability to analyse the sample in frozen state (so called frozen hydrated). Frozen hydrated analysis has shown to increase the signal of protonated ions, due to proton availability from the water matrix[217]. All samples in this thesis have been analyzed after freeze-drying.

ToF-SIMS analysis with ToF.SIMS 5

All ToF-SIMS experiments in the papers included in this thesis were performed using the industry standard ToF.SIMS 5 imaging instrument, IONTOF GmbH, using the imaging and the depth profiling mode. The instrument is equipped with a 25 KeV bismuth cluster ion gun for nanometer scale imaging along with a 10 keV C_{60}^+ sputter gun for depth profiling of organic

and inorganic materials. It is equipped with a gridless reflectron type TOF analyzer giving high secondary ion transmission with high mass resolution, a sample chamber with a 5-axis manipulator (x, y, z, rotation and tilt) for flexible navigation, a fast entry load-lock, charge compensation for the analysis of insulators, a secondary electron detector for SEM imaging, a state-of-the-art vacuum system, and an extensive computer package for automation and data handling.

Measurements modes with the ToF.SIMS 5

1. Surface spectrometry: surface spectrometry or static SIMS mode, elemental as well as molecular information about the chemical composition of the surface can be obtained with high sensitivity. In order to analyze the original surface (unchanged by the primary ion beam), the applied primary ion dose density is kept low enough that the contribution of already damaged surface areas can be neglected.
2. Imaging: For this mode, the primary ion beam is scanned over a defined surface area. At each pixel of the raster, a spectrum is recorded that can be assigned to a certain position on the sample surface. By selecting certain mass peaks out of the spectra, surface images can be generated for the corresponding species.
3. Depth profiling: depth profiling is performed in the dual beam mode. In this mode, sample erosion and analysis are performed by two different guns. A sputter gun is used to erode the surface (i.e. to generate the crater) and the analysis gun analyses an area in the center of the crater bottom. This principle allows adjustment of both ion guns independently for optimum conditions on a large variety of samples. Selected peak intensities or concentrations versus sputter time or depth can be displayed.
4. Secondary electron imaging: In addition to secondary ions, the ion bombardment of the sample surface leads to the emission of secondary electrons. The IONTOF V is equipped with a secondary electron detector, which allows to record images comparable to a scanning electron microscope. This mode is very helpful in cases where the mass analyzer cannot be used. A typical application is the initial alignment of the target deflection unit for the analysis gun prior to the adjustment of the analyzer ion optics.

Multivariate analysis

In order to generate data for one ToF-SIMS image, a large data set is acquired. For every pixel point in the image, a mass spectrum is generated. Each mass spectrum contains both background peaks and actual peaks, that could be very difficult to interpret, when it comes to biological tissues that contain large amounts of chemical information. Extracting the biological relevant information from biological tissue can be challenging. Hence, the use of multivariate analysis techniques has become a necessity. Several multivariate data analysis techniques have been applied and proved to be useful reducing the amount of ToF-SIMS data[218]. Of all the MVA methods, principal component analysis (PCA) is the most used. PCA transforms high-dimensions data into lower-dimensions, while retaining as much information as possible, by translating the data into a number of principal components. Thus, PCA attempts to explain as much variation as possible in as few components as possible. In ToF-SIMS data the relationships between the variables (m/z values) are presented in a score plot, and the corresponding loading (peak intensities) that give rise to the separation are presented in a loading plot. Before applying the PCA, the data needs to be pre-treated. Normalization of the ToF-SIMS data is important to minimize the variation due to sample charging, topography and/or instrumental conditions. A critical step in PCA is the data scaling, where each peak intensity (variable) is divided by the scaling factor. The scaling method influences how noise is separated from actual peaks.

Maximum auto correlation factor (MAF) is a PCA based multivariate analysis. It correlates the data to space domain in addition to m/z domain. MAF analysis produces better results for images than PCA, regarding subtle features and image contrast[218]. Moreover, MAF analysis is scaling independent, which makes it a more attractive option when analyzing images. The analysis procedure maximizes the autocorrelation between neighboring pixels where actual signal has high autocorrelation and noise has low correlation, with the assumption that noise in neighboring signal is similar.

PCA was applied in paper III, to detect changes in lipids owing to MI application to ex-vivo human skin. Data was normalized to total ion intensity, where the intensity of each peak was divided by total secondary ion intensity. The data were scaled using pareto scaling, dividing

each variable by the square root of the standard deviation. This helps to reduce the relative importance of large values, but keeps data structure partially intact[219].

MAF was applied in paper V to capture correlated spectral features arising from different parts of the samples features in two different human skin models, reconstruct human epidermis and ex-vivo human models.

Chapter 5

SUMMARY OF PAPERS

In paper I a study was performed to demonstrate the use of ToF-SIMS to monitor active substance penetration and localization through human skin tissue by studying sunscreen as one of many possible applications in the medical field. The method can serve as an alternative to artificial skin models and animal skin-based toxicology studies or product testing. Sunscreen is a term to describe products used to protect skin from UV light. They are usually administrated through topical routes which makes dermal penetration studies highly valuable. Chemical off-the-shelf sunscreen was applied to fresh frozen human skin using Franz type diffusion cells and imaged with a TOF.SIMS 5 imager, equipped with a bismuth liquid metal ion gun as a primary ion source and a C_{60}^+ ion source as a sputter source.

The study produced images that could be used to visualize the distribution of the chemical components of the sunscreens (Avobenzone, Bemotrizinol, Biscotrizole and Ethyl hexyl triazine), as well as endogenous skin substances such as fatty acids, cholesterol sulfate and phospholipids. Ion images, line scans as well as H&E images were used to investigate the penetration of the four substances. The chemical components showed different abilities to penetrate the skin depending on their structure and physicochemical properties but in general remained in the stratum corneum. An exception was seen with Avobenzone which penetrated into the dermis through a sebaceous gland. Similar results have been reported earlier in the literature using other techniques indicating that the model can be used to study skin permeation of active pharmaceutical compounds and other chemical compounds.

In the work presented in paper II, chromium, an element with complex chemistry and toxicity was investigated. Exposure to Cr^{VI} is an important risk factor for the development of lung cancer and can also cause allergic contact dermatitis. The aim of this study was to investigate the distribution and penetration of Cr^{VI} and Cr^{III} species in a reconstructed human epidermis (RHE) model comparing this to human skin *ex vivo*, focusing on skin uptake and distribution in

the skin tissue layers. Human skin and the RHE model were exposed to chromium prior to analysis by using Franz-Type diffusion cells.

The distribution of the metal (two valence states, Cr^{VI} and Cr^{III}) in the skin was imaged, using ToF.SIMS 5 imager, equipped with a bismuth liquid metal ion gun as a primary ion source and a C_{60} ion source as a sputter gun. In addition, the concentration of Cr^{VI} in donor and receptor fluids was measured to calculate the amount penetrated through the skin. The phosphatidylcholine head group fragment and cholesterol were used as markers to separate the stratum corneum from the epidermis. Line scan analysis was used to evaluate the difference in skin penetration of Cr^{VI} and Cr^{III} in the RHE model compared to human skin ex vivo.

Both Cr^{VI} and Cr^{III} penetrated into the reconstructed human epidermis layer corresponding to the stratum corneum; however, Cr^{VI} penetrated further in the tissue and was evenly distributed.

Compared to the ex-vivo human skin, the RHE model gave similar results for the penetration of Cr^{VI}. On the other hand, the penetration of Cr^{III} into the tissue differed markedly. In the RHE model the Cr^{III} species accumulated in the tissue layer corresponding to stratum corneum whereas in human skin *ex vivo*, the Cr^{III} species penetrated evenly through the skin tissue.

Analysis of Cr^{VI} concentrations in the donor fluids indicated no significant reduction to Cr^{III}. In the other hand, the Concentration of Cr^{VI} that were in direct contact with the human skin had about 50% reduction. This might indicate a reduction of Cr^{VI} due to the presence of certain biomolecules in skin, which are lacking or present in low abundance in the RHE mode. The percentage that penetrated the human skin ex vivo was less than the RHE model. This further supports that human skin ex vivo has a reduction capacity for Cr^{VI}, resulting in lower penetration rates.

Line scan analysis showed that the penetration pattern of Cr^{VI} into the skin is similar between the RHE model and the human skin ex vivo. In the other hand, the pattern of skin penetration of Cr^{III} is different between the two models. The RHE model indicates that Cr^{III} will not penetrate further than the layer corresponding to the stratum corneum, but the results from the human skin ex vivo indicate that Cr^{III} is able to penetrate into the epidermis.

Further, skin lipids such as cholesterol were less abundant in the RHE model compared to the human skin tissue. Results presented indicate that the RHE models do not possess the same fundamental properties as human skin tissue.

In paper III, MSI was used to follow the distribution of 2-methyl-4-isothiazolin-3-one (MI) in the skin using the concentration used in diagnostic patch-test and ToF-SIMS to investigate the uptake and the localization of MI in human ex-vivo skin tissue and follow possible lipid changes caused by it. (MI) is a low molecular weight (*m/z* 115) molecule used in an extensive variety of products including cosmetics, household detergents, paints, metalworking fluids, textiles and plastics. MI is associated with skin allergy. The incidence of contact allergy is decreased in Europe due to governmental regulation limiting concentrations of MI. However, incidence continues to rise in the USA.

MI was applied to ex-vivo human skin in accordance with the instructions supplied by the manufacturer and imaged with a TOF.SIMS 5 imager, equipped with a bismuth liquid metal ion gun as a primary ion source.

It was not possible to detect the pseudo molecular ion of the MI, hence an MI fragment *m/z* 63 was used to determine the substance distribution in the skin tissue. Ion images combined with line scans reveal an accumulation of MI in skin surface about 30-40 µm inside the skin, which represents the stratum corneum as well as the upper part of the viable epidermis. The MI exposed tissue showed a major increase in phosphatidylcholine and sphingomyelin lipids, and lower diacylglycerol content, indicating a direct effect of MI on skin lipids in the stratum corneum region. However, no apparent differences were observed in the viable epidermis between controls and MI-treated samples.

The aim of Paper IV was to gain a better understanding of similarity and differences between ex-vivo human skin and in-vitro human skin reconstructs via ToF-SIMS analysis, so that in future MSI analyses, more accurate data and interpretation of results can be done leading to relevant conclusions depending on which model is used.

The study of skin uptake and lipids changes in skin is of great interest in understanding underlying mechanisms of exposure to chemicals and environmental agents. Here I have utilized time of flight secondary ion mass spectrometry (ToF-SIMS) which is a powerful tool to

chemically map biological tissues and simultaneously localize both endogenous and exogenous compounds.

A reconstructed human skin was compared to an ex-vivo human skin by applying a TOF.SIMS 5 imager, equipped with a Bismuth cluster liquid metal ion gun as a primary ion source.

ToF-SIMS and subsequent MAF image analysis were successful in detecting different regions in both the ex-vivo and in-vitro skin tissues. The ex-vivo model resemble an actual human skin tissue biopsy, with respect to its size, appearance in the ToF-SIMS images, the distribution of the most detected lipids and lipids fragments in the tissue and thus the ionization and fragmentation pattern. The in-vitro skin tissue ion images do not closely resemble human skin in size, appearance, and the distribution of several important lipid fragments. Extra care should be taken when using the in-vitro skin model since it differs much from actual human skin.

CONCLUDING REMARKS AND FUTURE OUTLOOKS

ToF-SIMS imaging is a well-established technique and routinely used in inorganic material analysis in the semiconductor and coating industries. Over the years, ToF-SIMS instruments have undergone significant advancements. The new designs of mass analyzers as well as the development of ion sources offers extraordinarily high spatial resolution and sensitivity. Owing to these improvements, and its unique ability to carry out label-free localization of molecules across a sample surface, ToF-SIMS has become a powerful tool for various applications in the life sciences. ToF-SIMS can be used to image biological samples at the cellular and even subcellular level.

In this thesis work, it was shown that ToF-SIMS can be used to probe multiple compounds in biological tissues while being able to also trace the endogenous molecules in that tissue in the same run without labelling. This was demonstrated by studying how different active ingredients in sunscreen permeate through human skin. The uptake and subcellular location of multiple active ingredients of the sunscreen have been revealed. ToF-SIMS ion imaging was also used to detect the appendageal permeation pathway of the active ingredient, avobenzone.

It was also shown that ToF-SIMS can be used to trace metals and localize them at the subcellular level by studying the permeation of chromium III and chromium VI through different layers of the skin. The application of ToF-SIMS to study the uptake of the methylisothiazolinone allergen demonstrates that ToF-SIMS can be used to detect and localize low molecular organics, in addition to the ability to investigate lipidomics. An evaluation of skin models using ToF-SIMS was carried out as an application of using lipidomics to differentiate between different tissues and different sublayers in each tissue.

The ToF-SIMS methods developed, and the results obtained in this thesis demonstrate that ToF-SIMS can be used to study any metal or chemical permeation pathways, including the appendageal pathway, through all skin layers and sublayers. In addition, the effect of the penetrated substance on skin lipids in the different layers can also be detected. The method

developed here can be used to provide basis for creating correct limiting values for harmful levels of substances that can come into contact with the skin. In order to develop the maximum values for chemical exposure, one must know how much of the dose on the skin surface penetrates into and through the skin. This approach could also be used to study drug uptake in skin tissue as a complementary technique. Moreover, applying this method can replace the use of animals in drug development and toxicological studies.

In conclusion the ToF-SIMS method, with the strategies discussed in this thesis, is ready to be routinely used in testing pharmaceuticals, cosmetics, occupational skin hazards and skin allergens independently or as a complementary approach to answer other complicated scientific questions, including transdermal drug delivery, drug transport to the outer surface of the skin for sampling and monitoring, etc.

ACKNOWLEDGEMENTS

My PhD has been one of the greatest challenges of my life. I would like to express my deepest gratitude to the exceptional individuals who supported and guided me throughout this journey, enabling me to successfully obtain my PhD despite the many unforeseen obstacles that arose.

First of all, I would like to thank my supervisors:
Per Malmberg. Thank you for taking me as your Ph.D. student, encouraging and believing in me and always being supportive, teaching me how to use the IONTOF and how to write papers. Your exceptional ethics are unmatched; without your help this wouldn't be possible. It has been a great honor and privilege to do my Ph.D. under your supervision, THANK YOU!

Andy Ewing. Thank you for your excellent consultation and guidance, your valuable comments and feedback helped me grow up in science. Thank you for all great discussions we have had.

To my current examiner Marica Ericsson, thank you for keeping me honest to the schedule. Your exceptional knowledge and advice are valuable asset to every Ph.D. student.

To my previous examiner, Stefan Hulth, you are an amazing man, thank you for great discussions and advices. You have beautiful soul; you gave me so much positivity.

To Marcus Tamas, your support in much needed times helped me through this challenge.

Thank you to all the co-authors for the papers included in this thesis. Big thanks to Lina Hagvall and Niamh O'Boyle, you made it possible for me to study human skin tissue.

To my previous office mates, Ibrahim, Xian and Tina, and Daisy Thank you for all the scientific discussions, chats, laughs and positivity.

To Mai, Shoko, Nhu, Neda, Soodi, Sanna, Anna, Johan, Amir and all the other colleagues for the good times we shared over coffee breaks and in the lab.

To my husband Mahboob my number one supporter and Kids (Lamise, Saleem and Ahmed) thank you for supporting, encouraging me and being so proud of me, “My mom is Scientist!”, was one of the main reasons that motivated me to fulfill my PhD studies. I wanted to be a good example for you and not give up. I am so lucky to have such loving husband and kids.

To my parents, brother and sisters. Thank you for taking care of the kids and all the cooked dinners, so I can focus on my research work. Zainab, thank you for all the supportive WhatsApp calls trying to keep me focused and back on track.

Osama and Robert, you did not get to live very long, but I hope you will be proud of this.

REFRENCES

1. D'Alvise J, Mortensen R, Hansen SH, Janfelt C. Detection of follicular transport of lidocaine and metabolism in adipose tissue in pig ear skin by DESI mass spectrometry imaging. *Anal Bioanal Chem*. 2014;406(15):3735-3742. doi:10.1007/s00216-014-7802-z

2. Malmberg P, Guttenberg T, Ericson MB, Hagvall L. Imaging mass spectrometry for novel insights into contact allergy – a proof-of-concept study on nickel. *Contact Dermatitis*. 2018;78(2):109-116. doi:10.1111/cod.12911

3. Zhang D, Bian Q, Zhou Y, Huang Q, Gao J. The application of label-free imaging technologies in transdermal research for deeper mechanism revealing. *Asian Journal of Pharmaceutical Sciences*. 2021;16(3):265-279. doi:10.1016/j.ajps.2020.07.004

4. Najafinobar N, Venkatesan S, von Sydow L, et al. ToF-SIMS mediated analysis of human lung tissue reveals increased iron deposition in COPD (GOLD IV) patients. *Sci Rep*. 2019;9(1):10060. doi:10.1038/s41598-019-46471-7

5. Lovászi M, Szegedi A, Zouboulis CC, Törőcsik D. Sebaceous-immunobiology is orchestrated by sebum lipids. *Dermato-Endocrinology*. 2017;9(1):e1375636. doi:10.1080/19381980.2017.1375636

6. Downing: Changes in sebum secretion and the sebaceous gland - Google Scholar. Accessed August 15, 2023. https://scholar.google.com/scholar_lookup?journal=Clin+Geriatr+Med&title=Changes+in+sebum+secretion+and+the+sebaceous+gland&author=DT+Downing&author=ME+Stewart&author=JS+Strauss&volume=5&publication_year=1989&pages=109-114&pmid=2645990&

7. Nygren H, Dahlén G, Malmberg P. Analysis of As- and Hg-Species in Metal-Resistant Oral Bacteria, by Imaging ToF-SIMS. *Basic & Clinical Pharmacology & Toxicology*. 2014;115(1):129-133. doi:10.1111/bcpt.12205

8. Hagvall L, Pour MD, Feng J, Karma M, Hedberg Y, Malmberg P. Skin permeation of nickel, cobalt and chromium salts in ex vivo human skin, visualized using mass spectrometry imaging. *Toxicology in Vitro*. 2021;76:105232.

9. Hagvall L, Munem M, Hoang Philipsen M, Dowlatshahi Pour M, Hedberg Y, Malmberg P. Skin permeation studies of chromium species – Evaluation of a reconstructed human epidermis model. *Toxicology in Vitro*. 2023;91:105636. doi:10.1016/j.tiv.2023.105636

10. Pakiet A, Kobiela J, Stepnowski P, Sledzinski T, Mika A. Changes in lipids composition and metabolism in colorectal cancer: a review. *Lipids in Health and Disease*. 2019;18(1):29. doi:10.1186/s12944-019-0977-8

11. Parhofer KG. Interaction between Glucose and Lipid Metabolism: More than Diabetic Dyslipidemia. *Diabetes Metab J*. 2015;39(5):353-362. doi:10.4093/dmj.2015.39.5.353

12. Erion DM, Park HJ, Lee HY. The role of lipids in the pathogenesis and treatment of type 2 diabetes and associated co-morbidities. *BMB Rep*. 2016;49(3):139-148. doi:10.5483/BMBRep.2016.49.3.268

13. Estes RE, Lin B, Khera A, Davis MY. Lipid Metabolism Influence on Neurodegenerative Disease Progression: Is the Vehicle as Important as the Cargo? *Front Mol Neurosci*. 2021;14:788695. doi:10.3389/fnmol.2021.788695

14. Alberts B, Johnson A, Lewis J, Raff M, Roberts K, Walter P. *Molecular Biology of the Cell*. 4th ed. Garland Science; 2002.

15. Your Web site for FATS and OILS. Accessed September 7, 2023. https://cyberlipid.gerli.com/

16. LIPID MAPS. Accessed September 7, 2023. https://www.lipidmaps.org/

17. LipidBank. Accessed September 7, 2023. https://lipidbank.jp/

18. Fahy: A comprehensive classification system for lipids1 - Google Scholar. Accessed September 7, 2023. https://scholar.google.com/scholar_lookup?journal=J+Lipid+Res&title=A+comprehensive+classification+system+for+lipids&author=E+Fahy&author=S+Subramaniam&author=HA+Brown&author=CK+Glass&author=AH+Merrill&volume=46&publication_year=2005&pages=839-861&pmid=15722563&

19. Fahy: Update of the LIPID MAPS comprehensive classificati... - Google Scholar. Accessed September 7, 2023. https://scholar.google.com/scholar_lookup?journal=J+Lipid+Res&title=Update+of+the+LIPID+MAPS+comprehensive+classification+system+for+lipids&author=E+Fahy&author=S+Subramaniam&author=RC+Murphy&author=CRH+Raetz&author=M+Nishijima&volume=50&issue=Suppl&publication_year=2009&pages=S9-S14&pmid=19098281&

20. Farese RV, Walther TC. Lipid Droplets Finally Get a Little R-E-S-P-E-C-T. *Cell*. 2009;139(5):855-860. doi:10.1016/j.cell.2009.11.005

21. Tauchi-Sato K, Ozeki S, Houjou T, Taguchi R, Fujimoto T. The Surface of Lipid Droplets Is a Phospholipid Monolayer with a Unique Fatty Acid Composition*. *Journal of Biological Chemistry*. 2002;277(46):44507-44512. doi:10.1074/jbc.M207712200

22. Eichmann TO, Lass A. DAG tales: the multiple faces of diacylglycerol—stereochemistry, metabolism, and signaling. *Cell Mol Life Sci*. 2015;72:3931-3952. doi:10.1007/s00018-015-1982-3

23. Kolczynska K, Loza-Valdes A, Hawro I, Sumara G. Diacylglycerol-evoked activation of PKC and PKD isoforms in regulation of glucose and lipid metabolism: a review. *Lipids in Health and Disease*. 2020;19(1):113. doi:10.1186/s12944-020-01286-8

24. D'Souza K, Epand RM. Enrichment of phosphatidylinositols with specific acyl chains. *Biochimica et Biophysica Acta (BBA) - Biomembranes*. 2014;1838(6):1501-1508. doi:10.1016/j.bbamem.2013.10.003

25. Vance JE. Phospholipid Synthesis and Transport in Mammalian Cells. *Traffic*. 2015;16(1):1-18. doi:10.1111/tra.12230

26. Bratton DL, Henson PM. Apoptotic cell recognition: will the real phosphatidylserine receptor(s) please stand up? *Curr Biol*. 2008;18(2):R76-79. doi:10.1016/j.cub.2007.11.024

27. Intracellular Signaling by Hydrolysis of Phospholipids and Activation of Protein Kinase C. doi:10.1126/science.1411571

28. Vance JE, Tasseva G. Formation and function of phosphatidylserine and phosphatidylethanolamine in mammalian cells. *Biochimica et Biophysica Acta (BBA) - Molecular and Cell Biology of Lipids*. 2013;1831(3):543-554. doi:10.1016/j.bbalip.2012.08.016

29. Merrill AH. CHAPTER 13 - Sphingolipids. In: Vance DE, Vance JE, eds. *Biochemistry of Lipids, Lipoproteins and Membranes (Fifth Edition)*. Elsevier; 2008:363-397. doi:10.1016/B978-044453219-0.50015-5

30. Ruvolo PP. Ceramide regulates cellular homeostasis via diverse stress signaling pathways. *Leukemia*. 2001;15(8):1153-1160. doi:10.1038/sj.leu.2402197

31. Kolesnick R. The therapeutic potential of modulating the ceramide/sphingomyelin pathway. *J Clin Invest*. 2002;110(1):3-8. doi:10.1172/JCI16127

32. Coderch L, López O, de la Maza A, Parra JL. Ceramides and skin function. *Am J Clin Dermatol*. 2003;4(2):107-129. doi:10.2165/00128071-200304020-00004

33. Draelos ZD. The effect of ceramide-containing skin care products on eczema resolution duration. *Cutis*. 2008;81(1):87-91.

34. Morad SAF, Cabot MC. Ceramide-orchestrated signalling in cancer cells. *Nat Rev Cancer*. 2013;13(1):51-65. doi:10.1038/nrc3398

35. Hammerschmidt P, Brüning JC. Contribution of specific ceramides to obesity-associated metabolic diseases. *Cell Mol Life Sci*. 2022;79(8):395. doi:10.1007/s00018-022-04401-3

36. Gaggini M, Ndreu R, Michelucci E, Rocchiccioli S, Vassalle C. Ceramides as Mediators of Oxidative Stress and Inflammation in Cardiometabolic Disease. *Int J Mol Sci*. 2022;23(5):2719. doi:10.3390/ijms23052719

37. Chakraborty M, Jiang XC. Sphingomyelin and Its Role in Cellular Signaling. *Advances in experimental medicine and biology*. 2013;991:1-14. doi:10.1007/978-94-007-6331-9_1

38. Hannich JT, Umebayashi K, Riezman H. Distribution and Functions of Sterols and Sphingolipids. *Cold Spring Harb Perspect Biol*. 2011;3(5):a004762. doi:10.1101/cshperspect.a004762

39. Rahmati-Ahmadabad S, Broom DR, Ghanbari-Niaki A, Shirvani H. Effects of exercise on reverse cholesterol transport: A systemized narrative review of animal studies. *Life Sci*. 2019;224:139-148. doi:10.1016/j.lfs.2019.03.058

40. Plat J, Baumgartner S, Vanmierlo T, et al. Plant-based sterols and stanols in health & disease: "Consequences of human development in a plant-based environment?" *Prog Lipid Res*. 2019;74:87-102. doi:10.1016/j.plipres.2019.02.003

41. Ding X, Zhang W, Li S, Yang H. The role of cholesterol metabolism in cancer. *Am J Cancer Res*. 2019;9(2):219-227.

42. Goldsmith: Physiology, biochemistry, and molecular... - Google Scholar. Accessed August 15, 2023. https://scholar.google.com/scholar_lookup?title=Physiology,+Biochemistry+and+Molecular+Biology+of+the+Skin&author=JS+Strauss&author=DT+Downing&author=JF+Ebling&author=ME+Stewart&publication_year=1991&

43. Smith: Thematic review series: skin lipids. Sebaceous... - Google Scholar. Accessed August 15, 2023. https://scholar.google.com/scholar_lookup?journal=J+Lipid+Res&title=Sebaceous+gland+lipids:+Fri

end+or+foe?&author=KR+Smith&author=DM+Thiboutot&volume=49&publication_year=2008&pages=271-281&pmid=17975220&

44. Elias: Lipids and the epidermal water barrier: metabolism... - Google Scholar. Accessed August 16, 2023. https://scholar.google.com/scholar_lookup?journal=Semin+Dermatol&title=Lipids+and+the+epidermal+water+barrier:+Metabolism,+regulation+and+pathophysiology&author=PM+Elias&author=KR+Feingold&volume=11&publication_year=1992&pages=176-182&pmid=1498022&

45. Schurer NY, Elias PM. The Biochemistry and Function of Stratum Corneum Lipids. In: Elias PM, ed. *Advances in Lipid Research*. Vol 24. Skin Lipids. Elsevier; 1991:27-56. doi:10.1016/B978-0-12-024924-4.50006-7

46. Bhattacharya N, Sato WJ, Kelly A, Ganguli-Indra G, Indra AK. Epidermal Lipids: Key Mediators of Atopic Dermatitis Pathogenesis. *Trends in Molecular Medicine*. 2019;25(6):551-562. doi:10.1016/j.molmed.2019.04.001

47. Feingold KR. The outer frontier: the importance of lipid metabolism in the skin. *J Lipid Res*. 2009;50(Suppl):S417-S422. doi:10.1194/jlr.R800039-JLR200

48. Picardo: Sebaceous gland lipids - Google Scholar. Accessed August 16, 2023. https://scholar.google.com/scholar_lookup?hl=en&volume=1&publication_year=2009&pages=68-71&journal=Dermatoendocrinology&author=Picardo+M.&title=Sebaceous+gland+lipids

49. Haschek WM, Rousseaux CG, Wallig MA, eds. Copyright. In: *Handbook of Toxicologic Pathology (Second Edition)*. Academic Press; 2002:iv. doi:10.1016/B978-0-12-330215-1.50048-X

50. Drakou K, Tsianni A, Vrani F, Kefala V, Rallis E. Revealing the Correlation between Altered Skin Lipids Composition and Skin Disorders. *Cosmetics*. 2021;8(3):88. doi:10.3390/cosmetics8030088

51. Knox S, O'Boyle NM. Skin lipids in health and disease: A review. *Chemistry and Physics of Lipids*. 2021;236:105055. doi:10.1016/j.chemphyslip.2021.105055

52. Lopez-Ojeda W, Pandey A, Alhajj M, Oakley AM. Anatomy, Skin (Integument). In: *StatPearls*. StatPearls Publishing; 2023. Accessed September 25, 2023. http://www.ncbi.nlm.nih.gov/books/NBK441980/

53. Bensouilah J, Buck P. *Aromadermatology: Aromatherapy in the Treatment and Care of Common Skin Conditions*. Radcliffe Publishing; 2006.

54. Hadgraft J. Skin, the final frontier. *International journal of pharmaceutics*. 2001;224(1-2):1-18.

55. Montagna W. *The Structure and Function of Skin*. Elsevier; 2012.

56. Agarwal S, Krishnamurthy K. Histology, Skin. In: *StatPearls*. StatPearls Publishing; 2023. Accessed December 17, 2023. http://www.ncbi.nlm.nih.gov/books/NBK537325/

57. van Smeden J, Janssens M, Gooris GS, Bouwstra JA. The important role of stratum corneum lipids for the cutaneous barrier function. *Biochim Biophys Acta*. 2014;1841(3):295-313. doi:10.1016/j.bbalip.2013.11.006

58. Burns T, Breathnach SM, Cox N, Griffiths C. *Rook's Textbook of Dermatology*. John Wiley & Sons; 2008.

59. Kolimi P, Narala S, Nyavanandi D, Youssef AAA, Dudhipala N. Innovative Treatment Strategies to Accelerate Wound Healing: Trajectory and Recent Advancements. *Cells*. 2022;11(15):2439. doi:10.3390/cells11152439

60. Wertz P. Epidermal Lamellar Granules. *Skin Pharmacology and Physiology*. 2018;31(5):262-268. doi:10.1159/000491757

61. Muhammad F, Riviere JE. Chapter 21 - Dermal toxicity. In: Gupta RC, ed. *Veterinary Toxicology (Second Edition)*. Academic Press; 2012:337-350. doi:10.1016/B978-0-12-385926-6.00021-1

62. Biga LM, Bronson S, Dawson S, et al. 5.1 Layers of the Skin. Published online September 26, 2019. Accessed November 1, 2023. https://open.oregonstate.education/aandp/chapter/5-1-layers-of-the-skin/

63. Anatomy of the Skin | SEER Training. Accessed November 1, 2023. https://training.seer.cancer.gov/melanoma/anatomy/

64. Scheuplein RJ, Blank IH. Permeability of the skin. *Physiological Reviews*. 1971;51(4):702-747. doi:10.1152/physrev.1971.51.4.702

65. Oesch F, Fabian E, Guth K, Landsiedel R. Xenobiotic-metabolizing enzymes in the skin of rat, mouse, pig, guinea pig, man, and in human skin models. *Arch Toxicol*. 2014;88(12):2135-2190. doi:10.1007/s00204-014-1382-8

66. Roberts MS, Cross SE, Anissimov YG. Factors Affecting the Formation of a Skin Reservoir for Topically Applied Solutes. *Skin Pharmacology and Applied Skin Physiology*. 2003;17(1):3-16. doi:10.1159/000074057

67. Guy RH, Hadgraft J, Bucks DA. Transdermal drug delivery and cutaneous metabolism. *Xenobiotica*. 1987;17(3):325-343. doi:10.3109/00498258709043943

68. Grandjean P. *Skin Penetration: Hazardous Chemicals At Work*. Taylor & Francis; 1990.

69. Follicles play an important role in percutaneous absorption - Illel - 1991 - Journal of Pharmaceutical Sciences - Wiley Online Library. Accessed October 19, 2023. https://onlinelibrary.wiley.com/doi/abs/10.1002/jps.2600800505

70. Schneider M, Stracke F, Hansen S, Schaefer UF. Nanoparticles and their interactions with the dermal barrier. *Dermato-Endocrinology*. 2009;1(4):197-206. doi:10.4161/derm.1.4.9501

71. Sala M, Diab R, Elaissari A, Fessi H. Lipid nanocarriers as skin drug delivery systems: Properties, mechanisms of skin interactions and medical applications. *International Journal of Pharmaceutics*. 2018;535(1):1-17. doi:10.1016/j.ijpharm.2017.10.046

72. Yoshida K, Yokouchi M, Nagao K, Ishii K, Amagai M, Kubo A. Functional tight junction barrier localizes in the second layer of the stratum granulosum of human epidermis. *Journal of Dermatological Science*. 2013;71(2):89-99. doi:10.1016/j.jdermsci.2013.04.021

73. Structure and function of the stratum corneum permeability barrier - Elias - 1988 - Drug Development Research - Wiley Online Library. Accessed December 17, 2023. https://onlinelibrary.wiley.com/doi/abs/10.1002/ddr.430130203

74. Gaspari AA, Tyring SK, Kaplan DH. *Clinical and Basic Immunodermatology*. Springer; 2017.

75. Sonkoly E, Muller A, Lauerma AI, et al. IL-31: A new link between T cells and pruritus in atopic skin inflammation. *Journal of Allergy and Clinical Immunology*. 2006;117(2):411-417. doi:10.1016/j.jaci.2005.10.033

76. Dillon SR, Sprecher C, Hammond A, et al. Interleukin 31, a cytokine produced by activated T cells, induces dermatitis in mice. *Nat Immunol*. 2004;5(7):752-760. doi:10.1038/ni1084

77. Lauerma A, Werner P, Wisgrill L, Fyhrquist N. New Key Players in Irritant Contact Dermatitis: Residential Skin Cells and Neutrophils Drive Inflammation. *Journal of Investigative Dermatology*. 2022;142(3, Part A):509-512. doi:10.1016/j.jid.2021.09.002

78. Beck LA, Cork MJ, Amagai M, et al. Type 2 Inflammation Contributes to Skin Barrier Dysfunction in Atopic Dermatitis. *JID Innovations*. 2022;2(5). doi:10.1016/j.xjidi.2022.100131

79. De Benedetto: Histamine and skin barrier: are histamine... - Google Scholar. Accessed December 17, 2023. https://scholar.google.com/scholar_lookup?hl=en&volume=4&publication_year=2015&pages=741-755&journal=J%C2%A0Clin+Med&author=De+Benedetto+A.&author=Yoshida+T.&author=Fridy+S.&author=Park+J.E.&author=Kuo+I.H.&author=Beck+L.A.&title=Histamine+and+skin+barrier%3A+are+histamine+antagonists+useful+for+the+prevention+or+treatment+of+atopic+dermatitis%3F

80. Gschwandtner: Histamine suppresses epidermal keratinocyte... - Google Scholar. Accessed December 17, 2023. https://scholar.google.com/scholar_lookup?hl=en&volume=68&publication_year=2013&pages=37-47&journal=Allergy&author=Gschwandtner+M.&author=Mildner+M.&author=Mlitz+V.&author=Gruber+F.&author=Eckhart+L.&author=Werfel+T.&title=Histamine+suppresses+epidermal+keratinocyte+differentiation+and+impairs%C2%A0skin+barrier+function+in+a+human+skin+model

81. Martins RM, Siqueira S, Fonseca MJV, Freitas LAP. Skin penetration and photoprotection of topical formulations containing benzophenone-3 solid lipid microparticles prepared by the solvent-free spray-congealing technique. *Journal of Microencapsulation*. 2014;31(7):644-653. doi:10.3109/02652048.2014.911378

82. Harris DC. *Quantitative Chemical Analysis*. 8th ed. W.H. Freeman and Co; 2010.

83. Li CC, Lin YT, Chen YT, Sie SF, Chen-Yang YW. Improvement in UV protection retention capability and reduction in skin penetration of benzophenone-3 with mesoporous silica as drug carrier by encapsulation. *Journal of Photochemistry and Photobiology B: Biology*. 2015;148:277-283. doi:10.1016/j.jphotobiol.2015.04.027

84. Puglia C, Damiani E, Offerta A, et al. Evaluation of nanostructured lipid carriers (NLC) and nanoemulsions as carriers for UV-filters: Characterization, in vitro penetration and photostability studies. *European Journal of Pharmaceutical Sciences*. 2014;51:211-217. doi:10.1016/j.ejps.2013.09.023

85. Haque T, Crowther JM, Lane ME, Moore DJ. Chemical ultraviolet absorbers topically applied in a skin barrier mimetic formulation remain in the outer stratum corneum of porcine skin. *International Journal of Pharmaceutics*. 2016;510(1):250-254. doi:10.1016/j.ijpharm.2016.06.041

86. Lademann J, Jacobi U, Surber C, Weigmann HJ, Fluhr JW. The tape stripping procedure – evaluation of some critical parameters. *European Journal of Pharmaceutics and Biopharmaceutics*. 2009;72(2):317-323. doi:10.1016/j.ejpb.2008.08.008

87. Tape stripping of human stratum corneum yields cell layers that originate from various depths because of furrows in the skin - Google Search. Accessed November 22, 2023.

https://www.google.com/search?q=Tape+stripping+of+human+stratum+corneum+yields+cell+layers+that+originate+from+various+depths+because+of+furrows+in+the+skin&rlz=1C1FKPE_svSE1044SE1044&oq=Tape+stripping+of+human+stratum+corneum+yields+cell+layers+that+originate+from+various+depths+because+of+furrows+in+the+skin&gs_lcrp=EgZjaHJvbWUyBggAEEUYOdIBBzc5N2owajeoAgCwAgA&sourceid=chrome&ie=UTF-8

88. Van Lierde V, Chéry CC, Roche N, Monstrey S, Moens L, Vanhaecke F. In vitro permeation of chromium species through porcine and human skin as determined by capillary electrophoresis-inductively coupled plasma-sector field mass spectrometry. *Anal Bioanal Chem*. 2006;384(2):378-384. doi:10.1007/s00216-005-0226-z

89. Midander K, Schenk L, Julander A. A novel approach to monitor skin permeation of metals in vitro. *Regulatory Toxicology and Pharmacology*. 2020;115:104693. doi:10.1016/j.yrtph.2020.104693

90. Tao H, Nagano K, Tasaki I, et al. Development and Evaluation of a System for the Semi-Quantitative Determination of the Physical Properties of Skin After Exposure to Silver Nanoparticles. *Nanoscale Res Lett*. 2020;15(1):187. doi:10.1186/s11671-020-03421-x

91. Chokshi RJ, Zia H, Sandhu HK, Shah NH, Malick WA. Improving the Dissolution Rate of Poorly Water Soluble Drug by Solid Dispersion and Solid Solution—Pros and Cons. *Drug Delivery*. 2007;14(1):33-45. doi:10.1080/10717540600640278

92. Jacobi U, Toll R, Sterry W, Lademann J. Do follicles play a role as penetration pathways in in vitro studies on porcine skin?- : An optical study. *Laser Physics*. Published online 2005. Accessed November 21, 2023. https://www.semanticscholar.org/paper/Do-follicles-play-a-role-as-penetration-pathways-in-Jacobi-Toll/f76a38a89d82abd09cce6db5aba0924325e10a97

93. Advanced chemical imaging and comparison of human and porcine hair follicles for drug delivery by confocal Raman microscopy. Accessed November 21, 2023. https://www.spiedigitallibrary.org/journals/journal-of-biomedical-optics/volume-18/issue-06/061210/Advanced-chemical-imaging-and-comparison-of-human-and-porcine-hair/10.1117/1.JBO.18.6.061210.full

94. Bodzon-Kulakowska A, Suder P. Imaging mass spectrometry: Instrumentation, applications, and combination with other visualization techniques. *Mass Spectrom Rev*. 2016;35(1):147-169. doi:10.1002/mas.21468

95. Hanrieder J, Malmberg P, Ewing AG. Spatial neuroproteomics using imaging mass spectrometry. *Biochimica et Biophysica Acta (BBA) - Proteins and Proteomics*. 2015;1854(7):718-731. doi:10.1016/j.bbapap.2014.12.026

96. Munem M, Zaar O, Dimovska Nilsson K, Neittaanmäki N, Paoli J, Fletcher JS. Chemical imaging of aggressive basal cell carcinoma using time-of-flight secondary ion mass spectrometry. *Biointerphases*. 2018;13(3):03B402. doi:10.1116/1.5016254

97. Starr NJ, Johnson DJ, Wibawa J, et al. Age-Related Changes to Human Stratum Corneum Lipids Detected Using Time-of-Flight Secondary Ion Mass Spectrometry Following in Vivo Sampling. *Anal Chem*. 2016;88(8):4400-4408. doi:10.1021/acs.analchem.5b04872

98. Sjövall P, Skedung L, Gregoire S, Biganska O, Clément F, Luengo GS. Imaging the distribution of skin lipids and topically applied compounds in human skin using mass spectrometry. *Sci Rep*. 2018;8(1):16683. doi:10.1038/s41598-018-34286-x

99. Avci: Animal models of skin disease for drug discovery - Google Scholar. Accessed August 15, 2023. https://scholar.google.com/scholar_lookup?title=Animal+models+of+skin+disease+for+drug+discov

ery&author=Avci,+P.&author=Sadasivam,+M.&author=Gupta,+A.&author=Melo,+W.&author=Huang,+Y.-
Y.&author=Yin,+R.&author=Chandran,+R.&author=Kumar,+R.&author=Otufowora,+A.&author=Nyame,+T.&publication_year=2013&journal=Expert+Opin.+Drug+Discov.&volume=8&pages=331%E2%80%93355&doi=10.1517/17460441.2013.761202

100. Jung: Animal models for percutaneous absorption - Google Scholar. Accessed August 15, 2023. https://scholar.google.com/scholar_lookup?title=Animal+models+for+percutaneous+absorption&author=Jung,+E.C.&author=Maibach,+H.I.&publication_year=2015&journal=J.+Appl.+Toxicol.&volume=35&pages=1%E2%80%9310&doi=10.1002/jat.3004

101. Dellambra: Non-animal models in dermatological research - Google Scholar. Accessed August 15, 2023. https://scholar.google.com/scholar_lookup?title=Non-animal+models+in+dermatological+research&author=Dellambra,+E.&author=Odorisio,+T.&author=D%E2%80%99Arcangelo,+D.&author=Failla,+C.M.&author=Facchiano,+A.&publication_year=2019&journal=ALTEX&volume=36&pages=177%E2%80%93202&doi=10.14573/altex.1808022

102. Pistollato F, Madia F, Corvi R, et al. Current EU regulatory requirements for the assessment of chemicals and cosmetic products: challenges and opportunities for introducing new approach methodologies. *Arch Toxicol*. 2021;95(6):1867-1897. doi:10.1007/s00204-021-03034-y

103. Rasmussen C, Gratz K, Liebel F, et al. The StrataTest® human skin model, a consistent in vitro alternative for toxicological testing. *Toxicology in Vitro*. 2010;24(7):2021-2029. doi:10.1016/j.tiv.2010.07.027

104. Küchler S, Strüver K, Friess W. Reconstructed skin models as emerging tools for drug absorption studies. *Expert Opinion on Drug Metabolism & Toxicology*. 2013;9(10):1255-1263. doi:10.1517/17425255.2013.816284

105. Human skin models: From healthy to disease-mimetic systems; characteristics and applications - Moniz - 2020 - British Journal of Pharmacology - Wiley Online Library. Accessed December 8, 2023. https://bpspubs.onlinelibrary.wiley.com/doi/10.1111/bph.15184

106. Lei X hua, Ning L na, Cao Y jing, et al. NASA-Approved Rotary Bioreactor Enhances Proliferation of Human Epidermal Stem Cells and Supports Formation of 3D Epidermis-Like Structure. *PLOS ONE*. 2011;6(11):e26603. doi:10.1371/journal.pone.0026603

107. Montaño I, Schiestl C, Schneider J, et al. Formation of human capillaries in vitro: the engineering of prevascularized matrices. *Tissue Eng Part A*. 2010;16(1):269-282. doi:10.1089/ten.TEA.2008.0550

108. Perez-Valle A, Del Amo C, Andia I. Overview of Current Advances in Extrusion Bioprinting for Skin Applications. *International Journal of Molecular Sciences*. 2020;21(18):6679. doi:10.3390/ijms21186679

109. Flaten GE, Palac Z, Engesland A, Filipović-Grčić J, Vanić Ž, Škalko-Basnet N. In vitro skin models as a tool in optimization of drug formulation. *European Journal of Pharmaceutical Sciences*. 2015;75:10-24. doi:10.1016/j.ejps.2015.02.018

110. Steinstraesser L, Rittig A, Gevers K, et al. A Human Full-Skin Culture System for Interventional Studies. *Eplasty*. 2009;9:e5.

111. Altelaar AFM, Luxembourg SL, McDonnell LA, Piersma SR, Heeren RMA. Imaging mass spectrometry at cellular length scales. *Nat Protoc*. 2007;2(5):1185-1196. doi:10.1038/nprot.2007.117

112. Bhardwaj C, Hanley L. Ion sources for mass spectrometric identification and imaging of molecular species. *Nat Prod Rep*. 2014;31(6):756-767. doi:10.1039/C3NP70094A

113. Fuchs B, Süss R, Schiller J. An update of MALDI-TOF mass spectrometry in lipid research. *Prog Lipid Res*. 2010;49(4):450-475. doi:10.1016/j.plipres.2010.07.001

114. Murphy RC, Hankin JA, Barkley RM. Imaging of lipid species by MALDI mass spectrometry. *J Lipid Res*. 2009;50(Suppl):S317-S322. doi:10.1194/jlr.R800051-JLR200

115. Sullards MC, Chen Y, Liu Y, Merrill AH. Imaging of lipids directly from brain tissue via matrix assisted laser desorption ionization Time-of-Flight Mass Spectrometry (MALDI TOF MS). *J Neurochem*. 2010;113.

116. Dill AL, Ifa DR, Manicke NE, Ouyang Z, Cooks RG. Mass spectrometric imaging of lipids using desorption electrospray ionization. *J Chromatogr B Analyt Technol Biomed Life Sci*. 2009;877(26):2883-2889. doi:10.1016/j.jchromb.2008.12.058

117. Ifa DR, Wiseman JM, Song Q, Cooks RG. Development of capabilities for imaging mass spectrometry under ambient conditions with desorption electrospray ionization (DESI). *International Journal of Mass Spectrometry*. 2007;1-3(259):8-15. doi:10.1016/j.ijms.2006.08.003

118. Manicke NE, Nefliu M, Wu C, et al. Imaging of lipids in atheroma by desorption electrospray ionization mass spectrometry. *Anal Chem*. 2009;81(21):8702-8707. doi:10.1021/ac901739s

119. Vickerman JC. Molecular imaging and depth profiling by mass spectrometry—SIMS, MALDI or DESI? *Analyst*. 2011;136(11):2199-2217. doi:10.1039/C1AN00008J

120. Bruinen AL, van Oevelen C, Eijkel GB, Van Heerden M, Cuyckens F, Heeren RMA. Mass Spectrometry Imaging of Drug Related Crystal-Like Structures in Formalin-Fixed Frozen and Paraffin-Embedded Rabbit Kidney Tissue Sections. *J Am Soc Mass Spectrom*. 2016;27(1):117-123. doi:10.1007/s13361-015-1254-3

121. Benabdellah F, Seyer A, Quinton L, Touboul D, Brunelle A, Laprévote O. Mass spectrometry imaging of rat brain sections: nanomolar sensitivity with MALDI versus nanometer resolution by TOF-SIMS. *Anal Bioanal Chem*. 2010;396(1):151-162. doi:10.1007/s00216-009-3031-2

122. Eberlin LS, Liu X, Ferreira CR, Santagata S, Agar NYR, Cooks RG. Desorption Electrospray Ionization then MALDI Mass Spectrometry Imaging of Lipid and Protein Distributions in Single Tissue Sections. *Anal Chem*. 2011;83(22):8366-8371. doi:10.1021/ac202016x

123. Benninghoven A. Surface analysis by Secondary Ion Mass Spectrometry (SIMS). *Surface Science*. 1994;299-300:246-260. doi:10.1016/0039-6028(94)90658-0

124. Sigmund P. Theory of Sputtering. I. Sputtering Yield of Amorphous and Polycrystalline Targets. *Phys Rev*. 1969;184(2):383-416. doi:10.1103/PhysRev.184.383

125. Behrisch R, Eckstein W. Sputtering by Particle Bombardment, Experiments and Computer Calculations from Threshold to MeV Energies. In: ; 2007. Accessed November 13, 2023. https://www.semanticscholar.org/paper/Sputtering-by-Particle-Bombardment%2C-Experiments-and-Behrisch-Eckstein/42dacd909f0aa5427a8e5b14ce4fb54bbef47c23

126. Vickerman JC. Secondary ion mass spectrometry-basic concepts, instrumental aspects, applications and trends. A. BENNINGHOVEN, F. G. RUDENAUER and H. W. WERNER, Wiley, New York, 1987, 1277 pages. *Surf Interface Anal*. 1987;10(8):435-435. doi:10.1002/sia.740100811

127. Cupak C, Szabo PS, Biber H, et al. Sputter yields of rough surfaces: Importance of the mean surface inclination angle from nano- to microscopic rough regimes. *Applied Surface Science*. 2021;570:151204. doi:10.1016/j.apsusc.2021.151204

128. TOF-SIMS: Materials Analysis by Mass Spectrometry 2nd Edn. Accessed October 24, 2023. https://www.impopen.com/store/TOF-SIMS-Materials-Analysis-by-Mass-Spectrometry-2nd-Edn-p513374510

129. Joo S, Liang H. Secondary Ion Mass Spectroscopy (SIMS). In: Wang QJ, Chung YW, eds. *Encyclopedia of Tribology*. Springer US; 2013:2989-2994. doi:10.1007/978-0-387-92897-5_1218

130. Williams P. On mechanisms of sputtered ion emission. *Applications of Surface Science*. 1982;13(1):241-259. doi:10.1016/0378-5963(82)90030-7

131. S˘roubek Z. Formation of ions in sputtering. *Spectrochimica Acta Part B: Atomic Spectroscopy*. 1989;44(3):317-328. doi:10.1016/0584-8547(89)80035-7

132. Wucher A. Formation of atomic secondary ions in sputtering. *Applied Surface Science*. 2008;255(4):1194-1200. doi:10.1016/j.apsusc.2008.05.252

133. Wittmaack K. Unravelling the secrets of Cs controlled secondary ion formation: Evidence of the dominance of site specific surface chemistry, alloying and ionic bonding. *Surface Science Reports*. 2013;68(1):108-230. doi:10.1016/j.surfrep.2012.11.001

134. Pachuta SJ, Cooks RG. Mechanisms in molecular SIMS. *Chem Rev*. 1987;87(3):647-669. doi:10.1021/cr00079a009

135. Storms HA, Brown KF, Stein JD. Evaluation of a cesium positive ion source for secondary ion mass spectrometry. *Anal Chem*. 1977;49(13):2023-2030. doi:10.1021/ac50021a034

136. Maul J, Wittmaack K. Secondary ion emission from silicon and silicon oxide. *Surface Science*. 1975;47(1):358-369. doi:10.1016/0039-6028(75)90300-3

137. Benninghoven A. Developments in secondary ion mass spectroscopy and applications to surface studies. *Surface Science*. 1975;53(1):596-625. doi:10.1016/0039-6028(75)90158-2

138. Banerjee TEC Sujit. *Surface Analysis of Paper*. CRC Press; 2020. doi:10.1201/9780429279997

139. Wucher A, Tian H, Winograd N. A Mixed Cluster Ion Beam to Enhance the Ionization Efficiency in Molecular Secondary Ion Mass Spectrometry. *Rapid Commun Mass Spectrom*. 2014;28(4):396-400. doi:10.1002/rcm.6793

140. Sheraz née Rabbani S, Berrueta Razo I, Kohn T, Lockyer NP, Vickerman JC. Enhancing Ion Yields in Time-of-Flight-Secondary Ion Mass Spectrometry: A Comparative Study of Argon and Water Cluster Primary Beams. *Anal Chem*. 2015;87(4):2367-2374. doi:10.1021/ac504191m

141. Rabbani S, Barber AM, Fletcher JS, Lockyer NP, Vickerman JC. TOF-SIMS with argon gas cluster ion beams: a comparison with C60+. *Anal Chem*. 2011;83(10):3793-3800. doi:10.1021/ac200288v

142. Benninghoven A, Mueller A. Secondary ion yields near 1 for some chemical compounds. *Physics Letters A*. 1972;40(2):169-170. doi:10.1016/0375-9601(72)90844-4

143. Zhang J, Franzreb K, Aksyonov SA, Williams P. Mass Spectra and Yields of Intact Charged Biomolecules Ejected by Massive Cluster Impact for Bioimaging in a Time-of-Flight Secondary Ion Microscope. *Analytical Chemistry*. 2015;87(21):10779-10784. doi:10.1021/acs.analchem.5b01802

144. Weidtmann B, Duvenbeck A, Wucher A. Predicting secondary ion formation in molecular dynamics simulations of sputtering. *Applied Surface Science*. 2008;255(4):813-815. doi:10.1016/j.apsusc.2008.05.062

145. Grade H, Winograd N, Cooks RG. Cationization of organic molecules in secondary ion mass spectrometry. *J Am Chem Soc*. 1977;99(23):7725-7726. doi:10.1021/ja00465a062

146. Wu KJ, Odom RW. Matrix-enhanced secondary ion mass spectrometry: a method for molecular analysis of solid surfaces. *Anal Chem*. 1996;68(5):873-882. doi:10.1021/ac950717i

147. Kucher A, Wucher A, Winograd N. Strong Field Ionization of β-Estradiol in the IR: Strategies To Optimize Molecular Postionization in Secondary Neutral Mass Spectrometry. *J Phys Chem C*. 2014;118(44):25534-25544. doi:10.1021/jp5080708

148. Popczun NJ, Breuer L, Wucher A, Winograd N. On the SIMS Ionization Probability of Organic Molecules. *J Am Soc Mass Spectrom*. 2017;28(6):1182-1191. doi:10.1007/s13361-017-1624-0

149. Conlan XA, Lockyer NP, Vickerman JC. Is proton cationization promoted by polyatomic primary ion bombardment during time-of-flight secondary ion mass spectrometry analysis of frozen aqueous solutions? *Rapid Commun Mass Spectrom*. 2006;20(8):1327-1334. doi:10.1002/rcm.2446

150. Belu AM, Graham DJ, Castner DG. Time-of-flight secondary ion mass spectrometry: techniques and applications for the characterization of biomaterial surfaces. *Biomaterials*. 2003;24(21):3635-3653. doi:10.1016/S0142-9612(03)00159-5

151. Jones EA, Lockyer NP, Kordys J, Vickerman JC. Suppression and enhancement of secondary ion formation due to the chemical environment in static-secondary ion mass spectrometry. *J Am Soc Mass Spectrom*. 2007;18(8):1559-1567. doi:10.1016/j.jasms.2007.05.014

152. Fletcher JS, Vickerman JC. A new SIMS paradigm for 2D and 3D molecular imaging of bio-systems. *Anal Bioanal Chem*. 2010;396(1):85-104. doi:10.1007/s00216-009-2986-3

153. Denbigh JL, Lockyer NP. ToF-SIMS as a tool for profiling lipids in cancer and other diseases. *Materials Science and Technology*. 2015;31(2):137-147. doi:10.1179/1743284714Y.0000000648

154. Kraft ML, Klitzing HA. Imaging lipids with secondary ion mass spectrometry. *Biochim Biophys Acta*. 2014;1841(8):1108-1119. doi:10.1016/j.bbalip.2014.03.003

155. Giardina M, Cheong S, Marjo CE, et al. Quantifying Inorganic Nitrogen Assimilation by Synechococcus Using Bulk and Single-Cell Mass Spectrometry: A Comparative Study. *Frontiers in Microbiology*. 2018;9. Accessed November 10, 2023. https://www.frontiersin.org/articles/10.3389/fmicb.2018.02847

156. Peer Reviewed: Organic SIMS of Biologic Tissue. *Anal Chem*. 1997;69(17):529A-535A. doi:10.1021/ac971763g

157. Organic Mass Spectrometry. In: *Fundamentals of Contemporary Mass Spectrometry*. John Wiley & Sons, Ltd; 2007:195-261. doi:10.1002/9780470118498.ch6

158. Passarelli MK, Winograd N. Lipid imaging with time-of-flight secondary ion mass spectrometry (ToF-SIMS). *Biochim Biophys Acta*. 2011;1811(11):976-990. doi:10.1016/j.bbalip.2011.05.007

159. Gillen Greg, Bennett Joe, Tarlov MJ, Burgess DRF. Molecular Imaging Secondary Ion Mass Spectrometry for the Characterization of Patterned Self-Assembled Monolayers on Silver and Gold. *Anal Chem*. 1994;66(13):2170-2174. doi:10.1021/ac00085a036

160. Brummel CL, Lee IN, Zhou Y, Benkovic SJ, Winograd N. A mass spectrometric solution to the address problem of combinatorial libraries. *Science*. 1994;264(5157):399-402. doi:10.1126/science.8153627

161. Dickinson M, Heard PJ, Barker JHA, Lewis AC, Mallard D, Allen GC. Dynamic SIMS analysis of cryo-prepared biological and geological specimens. *Applied Surface Science*. 2006;252(19):6793-6796. doi:10.1016/j.apsusc.2006.02.236

162. Kaklamanos G, Aprea E, Theodoridis G. Mass Spectrometry: Principles and Instrumentation. In: Caballero B, Finglas PM, Toldrá F, eds. *Encyclopedia of Food and Health*. Academic Press; 2016:661-668. doi:10.1016/B978-0-12-384947-2.00447-5

163. Green FM, Gilmore IS, Seah MP. TOF-SIMS: Accurate mass scale calibration. *J Am Soc Mass Spectrom*. 2006;17(4):514-523. doi:10.1016/j.jasms.2005.12.005

164. Ens W, Standing KG. Hybrid Quadrupole/Time-of-Flight Mass Spectrometers for Analysis of Biomolecules. In: *Methods in Enzymology*. Vol 402. Biological Mass Spectrometry. Academic Press; 2005:49-78. doi:10.1016/S0076-6879(05)02002-1

165. Carado A, Passarelli MK, Kozole J, Wingate JE, Winograd N, Loboda AV. C60 SIMS with a Hybrid-Quadrupole Orthogonal time-of-flight Mass Spectrometer. *Anal Chem*. 2008;80(21):7921-7929. doi:10.1021/ac801712s

166. Passarelli MK, Pirkl A, Moellers R, et al. The 3D OrbiSIMS—label-free metabolic imaging with subcellular lateral resolution and high mass-resolving power. *Nat Methods*. 2017;14(12):1175-1183. doi:10.1038/nmeth.4504

167. Cameron AE, Eggers DF Jr. An Ion ``Velocitron''. *Review of Scientific Instruments*. 2004;19(9):605-607. doi:10.1063/1.1741336

168. Mamyrin BA, Karataev VI, Shmikk DV, Zagulin VA. Mass reflection: a new nonmagnetic time-of-flight high resolution mass- spectrometer. *Zh Eksp Teor Fiz 64: No 1, 82-89(Jan 1973)*. Published online January 1, 1973. Accessed November 19, 2023. https://www.osti.gov/biblio/4560209

169. Le Beyec Y. Cluster impacts at keV and MeV energies: Secondary emission phenomena. *International Journal of Mass Spectrometry and Ion Processes*. 1998;174(1):101-117. doi:10.1016/S0168-1176(97)00294-2

170. Weibel D, Wong S, Lockyer N, Blenkinsopp P, Hill R, Vickerman JC. A C60 Primary Ion Beam System for Time of Flight Secondary Ion Mass Spectrometry: Its Development and Secondary Ion Yield Characteristics. *Anal Chem*. 2003;75(7):1754-1764. doi:10.1021/ac026338o

171. Touboul D, Kollmer F, Niehuis E, Brunelle A, Laprévote O. Improvement of biological time-of-flight-secondary ion mass spectrometry imaging with a bismuth cluster ion source. *J Am Soc Mass Spectrom*. 2005;16(10):1608-1618. doi:10.1016/j.jasms.2005.06.005

172. Szakal C, Kozole J, Russo MF, Garrison BJ, Winograd N. Surface Sensitivity in Cluster-Ion-Induced Sputtering. *Phys Rev Lett*. 2006;96(21):216104. doi:10.1103/PhysRevLett.96.216104

173. Yamada I. Historical milestones and future prospects of cluster ion beam technology. *Applied Surface Science*. 2014;310:77-88. doi:10.1016/j.apsusc.2014.03.147

174. Yamada I, Matsuo J, Toyoda N, Kirkpatrick A. Materials processing by gas cluster ion beams. *Materials Science and Engineering: R: Reports*. 2001;34(6):231-295. doi:10.1016/S0927-796X(01)00034-1

175. Winograd N, Postawa Z, Cheng J, Szakal C, Kozole J, Garrison BJ. Improvements in SIMS continue: Is the end in sight? *Applied Surface Science*. 2006;252(19):6836-6843. doi:10.1016/j.apsusc.2006.02.142

176. Angerer TB, Blenkinsopp P, Fletcher JS. High energy gas cluster ions for organic and biological analysis by time-of-flight secondary ion mass spectrometry. *International Journal of Mass Spectrometry*. 2015;377:591-598. doi:10.1016/j.ijms.2014.05.015

177. Kozole J, Winograd N. Controlling energy deposition during the C60+ bombardment of silicon: The effect of incident angle geometry. *Applied Surface Science*. 2008;255(4):886-889. doi:10.1016/j.apsusc.2008.05.259

178. Seah MP. Universal Equation for Argon Gas Cluster Sputtering Yields. *J Phys Chem C*. 2013;117(24):12622-12632. doi:10.1021/jp402684c

179. Luxembourg SL, Mize TH, McDonnell LA, Heeren RMA. High-Spatial Resolution Mass Spectrometric Imaging of Peptide and Protein Distributions on a Surface. *Anal Chem*. 2004;76(18):5339-5344. doi:10.1021/ac049692q

180. Kiss A, Jungmann JH, Smith DF, Heeren RMA. Microscope mode secondary ion mass spectrometry imaging with a Timepix detector. *Rev Sci Instrum*. 2013;84(1):013704. doi:10.1063/1.4772396

181. Nygren H, Hagenhoff B, Malmberg P, Nilsson M, Richter K. Bioimaging TOF-SIMS: High resolution 3D imaging of single cells. *Microscopy Research and Technique*. 2007;70(11):969-974. doi:10.1002/jemt.20502

182. Brison J, Robinson MA, Benoit DSW, Muramoto S, Stayton PS, Castner DG. TOF-SIMS 3D Imaging of Native and Non-Native Species within HeLa Cells. *Anal Chem*. 2013;85(22):10869-10877. doi:10.1021/ac402288d

183. Graham DJ, Gamble LJ. Dealing with image shifting in 3D ToF-SIMS depth profiles. *Biointerphases*. 2018;13(6):06E402. doi:10.1116/1.5041740

184. Chughtai K, Jiang L, Greenwood TR, et al. Fiducial Markers for Combined 3-Dimensional Mass Spectrometric and Optical Tissue Imaging. *Anal Chem*. 2012;84(4):1817-1823. doi:10.1021/ac203373h

185. Atomic and Molecular Imaging at the Single-Cell Level with TOF-SIMS | Analytical Chemistry. Accessed December 11, 2023. https://pubs.acs.org/doi/10.1021/ac9701748

186. Gilmore IS. SIMS of organics—Advances in 2D and 3D imaging and future outlook. *Journal of Vacuum Science & Technology A*. 2013;31(5):050819. doi:10.1116/1.4816935

187. Gilmore IS, Heiles S, Pieterse CL. Metabolic Imaging at the Single-Cell Scale: Recent Advances in Mass Spectrometry Imaging. *Annu Rev Anal Chem (Palo Alto Calif)*. 2019;12(1):201-224. doi:10.1146/annurev-anchem-061318-115516

188. Passarelli MK, Ewing AG. Single-cell imaging mass spectrometry. *Curr Opin Chem Biol*. 2013;17(5):854-859. doi:10.1016/j.cbpa.2013.07.017

189. Wu K, Jia F, Zheng W, Luo Q, Zhao Y, Wang F. Visualization of metallodrugs in single cells by secondary ion mass spectrometry imaging. *J Biol Inorg Chem*. 2017;22(5):653-661. doi:10.1007/s00775-017-1462-3

190. Kaya I, Jennische E, Lange S, Malmberg P. Multimodal chemical imaging of a single brain tissue section using ToF-SIMS, MALDI-ToF and immuno/histochemical staining. *Analyst*. 2021;146(4):1169-1177. doi:10.1039/D0AN02172E

191. Passarelli MK, Newman CF, Marshall PS, et al. Single-Cell Analysis: Visualizing Pharmaceutical and Metabolite Uptake in Cells with Label-Free 3D Mass Spectrometry Imaging. *Anal Chem*. 2015;87(13):6696-6702. doi:10.1021/acs.analchem.5b00842

192. Phan NTN, Fletcher JS, Sjövall P, Ewing AG. ToF-SIMS imaging of lipids and lipid related compounds in Drosophila brain. *Surf Interface Anal*. 2014;46(Suppl 1):123-126. doi:10.1002/sia.5547

193. Sämfors S, Ståhlman M, Klevstig M, Borén J, Fletcher JS. Localised lipid accumulation detected in infarcted mouse heart tissue using ToF-SIMS. *International Journal of Mass Spectrometry*. 2019;437:77-86. doi:10.1016/j.ijms.2017.09.012

194. Angerer TB, Magnusson Y, Landberg G, Fletcher JS. Lipid Heterogeneity Resulting from Fatty Acid Processing in the Human Breast Cancer Microenvironment Identified by GCIB-ToF-SIMS Imaging. *Anal Chem*. 2016;88(23):11946-11954. doi:10.1021/acs.analchem.6b03884

195. Abbas I, Noun M, Touboul D, Sahali D, Brunelle A, Ollero M. Kidney Lipidomics by Mass Spectrometry Imaging: A Focus on the Glomerulus. *Int J Mol Sci*. 2019;20(7):1623. doi:10.3390/ijms20071623

196. Debois D, Bralet MP, Le Naour F, Brunelle A, Laprévote O. In situ lipidomic analysis of nonalcoholic fatty liver by cluster TOF-SIMS imaging. *Anal Chem*. 2009;81(8):2823-2831. doi:10.1021/ac900045m

197. Philipsen MH, Phan NTN, Fletcher JS, Malmberg P, Ewing AG. Mass Spectrometry Imaging Shows Cocaine and Methylphenidate Have Opposite Effects on Major Lipids in Drosophila Brain. *ACS Chem Neurosci*. 2018;9(6):1462-1468. doi:10.1021/acschemneuro.8b00046

198. Marzec ME, Rząca C, Moskal P, Stępień EŁ. Study of the influence of hyperglycemia on the abundance of amino acids, fatty acids, and selected lipids in extracellular vesicles using TOF-SIMS. *Biochem Biophys Res Commun*. 2022;622:30-36. doi:10.1016/j.bbrc.2022.07.020

199. Noun M, Akoumeh R, Abbas I. Cell and Tissue Imaging by TOF-SIMS and MALDI-TOF: An Overview for Biological and Pharmaceutical Analysis. *Microsc Microanal*. 2022;28(1):1-26. doi:10.1017/S1431927621013593

200. Song Z, Wang Z, Zhao H, et al. Metabolic fingerprinting of cell types in mouse skeletal muscle by combining TOF-SIMS with immunofluorescence staining. *Analyst*. 2020;145(21):6901-6909. doi:10.1039/D0AN00738B

201. Davies SK, Fearn S, Allsopp LP, et al. Visualizing Antimicrobials in Bacterial Biofilms: Three-Dimensional Biochemical Imaging Using TOF-SIMS. *mSphere*. 2017;2(4):10.1128/msphere.00211-17. doi:10.1128/msphere.00211-17

202. Malmberg P, Nygren H. Methods for the analysis of the composition of bone tissue, with a focus on imaging mass spectrometry (TOF-SIMS). *PROTEOMICS*. 2008;8(18):3755-3762. doi:10.1002/pmic.200800198

203. Henss A, Rohnke M, El Khassawna T, et al. Applicability of ToF-SIMS for monitoring compositional changes in bone in a long-term animal model. *Journal of The Royal Society Interface*. 2013;10(86):20130332. doi:10.1098/rsif.2013.0332

204. Kern C, Ray S, Gelinsky M, Bellew AT, Pirkl A, Rohnke M. New insights into ToF-SIMS imaging in osteoporotic bone research. *Biointerphases*. 2020;15(3):031005. doi:10.1116/6.0000051

205. Kern C, Jamous R, Khassawna TE, Rohnke M. Characterisation of Sr2+ mobility in osteoporotic rat bone marrow by cryo-ToF-SIMS and cryo-OrbiSIMS. *Analyst*. 2022;147(18):4141-4157. doi:10.1039/D2AN00913G

206. Raghavan L, Brown M, Michniak-Kohn B, Ng S, Sammeta S. In Vitro Release Tests as a Critical Quality Attribute in Topical Product Development. In: Langley N, Michniak-Kohn B, Osborne DW, eds. *The Role of Microstructure in Topical Drug Product Development*. AAPS Advances in the Pharmaceutical Sciences Series. Springer International Publishing; 2019:47-87. doi:10.1007/978-3-030-17355-5_2

207. Franz TJ. Percutaneous Absorption. On the Relevance of in Vitro Data. *Journal of Investigative Dermatology*. 1975;64(3):190-195. doi:10.1111/1523-1747.ep12533356

208. Klein RR, Heckart JL, Thakker KD. In Vitro Release Testing Methodology and Variability with the Vertical Diffusion Cell (VDC). *Dissolution Technol*. 2018;25(3):52-61. doi:10.14227/DT250318P52

209. Clowes HM, Scott RC, Heylings JR. Skin absorption: Flow-through or static diffusion cells. *Toxicology in Vitro*. 1994;8(4):827-830. doi:10.1016/0887-2333(94)90078-7

210. van de Sandt JJM, van Burgsteden JA, Cage S, et al. In vitro predictions of skin absorption of caffeine, testosterone, and benzoic acid: a multi-centre comparison study. *Regulatory Toxicology and Pharmacology*. 2004;39(3):271-281. doi:10.1016/j.yrtph.2004.02.004

211. Shimizu H. *Shimizu's Dermatology*. 2nd ed. Wiley-Blackwell; 2016. Accessed November 21, 2023. https://www.perlego.com/book/997618/shimizus-dermatology-pdf

212. Breitenstein D, Rommel CE, Stolwijk J, Wegener J, Hagenhoff B. The chemical composition of animal cells reconstructed from 2D and 3D ToF-SIMS analysis. *Applied Surface Science*. 2008;255(4):1249-1256. doi:10.1016/j.apsusc.2008.05.289

213. Chandra S, Morrison GH. Sample preparation of animal tissues and cell cultures for secondary ion mass spectrometry (SIMS) microscopy. *Biology of the Cell*. 1992;74(1):31-42. doi:10.1016/0248-4900(92)90006-M

214. Malm J, Giannaras D, Riehle MO, Gadegaard N, Sjövall P. Fixation and Drying Protocols for the Preparation of Cell Samples for Time-of-Flight Secondary Ion Mass Spectrometry Analysis. *Anal Chem*. 2009;81(17):7197-7205. doi:10.1021/ac900636v

215. Berman ESF, Fortson SL, Checchi KD, et al. Preparation of single cells for imaging/profiling mass spectrometry. *J Am Soc Mass Spectrom*. 2008;19(8):1230-1236. doi:10.1016/j.jasms.2008.05.006

216. Bich C, Havelund R, Moellers R, et al. Argon Cluster Ion Source Evaluation on Lipid Standards and Rat Brain Tissue Samples. *Anal Chem*. 2013;85(16):7745-7752. doi:10.1021/ac4009513

217. Roddy TP, Cannon DM, Ostrowski SG, Ewing AG, Winograd N. Proton Transfer in Time-of-Flight Secondary Ion Mass Spectrometry Studies of Frozen-Hydrated Dipalmitoylphosphatidylcholine. *Anal Chem*. 2003;75(16):4087-4094. doi:10.1021/ac026353t

218. Graham DJ, Castner DG. Multivariate Analysis of ToF-SIMS Data from Multicomponent Systems: The Why, When, and How. *Biointerphases*. 2012;7(1):49. doi:10.1007/s13758-012-0049-3

219. van den Berg RA, Hoefsloot HC, Westerhuis JA, Smilde AK, van der Werf MJ. Centering, scaling, and transformations: improving the biological information content of metabolomics data. *BMC Genomics*. 2006;7:142. doi:10.1186/1471-2164-7-142